Multiscale Optimization of Weav3D Lattice-Reinforced Composites for Lightweight Structural Design

Jainam Chetan Mehta

A thesis
submitted in partial fulfillment of the
requirements for the degree of

Master of Science in Aeronautics & Astronautics

University of Washington

2025

Committee:

Marco Salviato

Jeff Wollschlager

Program Authorized to Offer Degree:
Aeronautics & Astronautics

University of Washington

Abstract

Multiscale Optimization
of Weav3D Lattice-Reinforced Composites
for Lightweight Structural Design

Jainam Chetan Mehta

Chair of the Supervisory Committee:
Marco Salviato
Department of Aeronautics & Astronautics

This thesis evaluates the effectiveness of conventional optimization methods applied to lattice-reinforced composite structures, specifically panels manufactured using Weav3D technology. Weav3D integrates thermoplastic composite tapes into tailored lattice geometries, enabling strategic reinforcement placement. Material properties of the carbon fiber tapes were first experimentally characterized through mechanical testing on a universal testing machine (UTM), with strain fields measured using Digital Image Correlation (DIC). These validated properties served as inputs to a computational optimization framework using Altair HyperStudy for parameter exploration, Jpanel for generating homogenized orthotropic material models, and OptiStruct for finite element analysis. A Design of Experiments (DOE) based on Latin Hypercube Sampling (LHS) guided surrogate modeling and global optimization.

Results showed a consistent preference for warp-direction reinforcement under bending loads, with fill-direction material significantly reduced. The final optimized lattice-based configuration achieved a 21% reduction in mass compared to a continuous baseline panel, confirming that classical surrogate-based optimization techniques can effectively streamline composite design without compromising performance.

TABLE OF CONTENTS

LIST OF FIGURES

GLOSSARY

BENDING STIFFNESS: The resistance of a structural element to deformation under an applied bending moment.

CARBON FIBER: A strong, stiff, lightweight material consisting of fibers about 5–10 micrometers in diameter composed mostly of carbon atoms.

CLASSICAL LAMINATION THEORY (CLT): A methodology used to predict the macroscopic behavior of composite laminates based on the properties and orientation of individual plies.

COMPOSITE: A material made from a combination of two or more materials.

CONSTRAINTS: In an optimization problem, these are the limits placed on the responses that must be satisfied.

DEHOMOGENIZATION: The process of recovering local stresses and strains in individual phases of a composite material from global homogenized results.

DESIGN OF EXPERIMENTS (DOE): A systematic method to determine the relationship between factors affecting a process and the output of that process.

DESIGN VARIABLES: In an optimization problem, design variables are parameters that can be adjusted in the model.

DIGITAL IMAGE CORRELATION (DIC): An optical measurement technique that tracks speckle patterns on a specimen's surface to calculate full-field displacements and strains during testing.

EXTENSIBLE LATTICE SEQUENCE (ELS): A lattice reinforcement patterning strategy in which warp and fill tapes are varied systematically to tailor stiffness and strength distribution within a composite panel.

FILL: The transverse direction in a woven lattice structure, perpendicular to the warp direction.

FINITE ELEMENT ANALYSIS (FEA): A numerical method for solving problems of engineering and mathematical physics by dividing a complex structure into small, simple elements.

FULL FACTORIAL: A DOE approach where every combination of input parameter levels is tested. It provides complete coverage of the design space but can be computationally intensive.

GLOBAL RESPONSE SURFACE METHOD (GRSM): A surrogate-based optimization approach that approximates the objective function using a response surface built from DOE results.

HOMOGENIZATION: The process of deriving equivalent properties for a heterogeneous material that represent its overall mechanical behavior.

JPANEL: A custom software tool used to homogenize lattice definitions and convert them into PSHELL+MAT2 entries for FEA. It automates multiscale property calculation.

LATTICE STRUCTURE: A regularly repeating arrangement of structural elements forming a three-dimensional framework.

LATIN HYPERCUBE SAMPLING (LHS): A statistical method for generating a distribution of plausible collections of parameter values from a multidimensional distribution. It ensures uniform sampling of each variable across its entire range.

MAT2: A 2D material definition card in OptiStruct used for representing orthotropic properties in shell elements.

MATRIX: The continuous phase in a composite material that surrounds and supports the reinforcement material.

MESH: A network of interconnected elements used in FEA to model a physical structure.

MODULUS OF ELASTICITY (E): A measure of the stiffness of the material, defined as the ratio of stress to strain in the elastic region.

MULTISCALE ANALYSIS: An analysis approach that addresses material behavior at different length scales to efficiently model complex heterogeneous structures.

OBJECTIVES: In an optimization problem, these values are the single response of the model to be maximized or minimized, such as the mass.

OPTIMIZATION: The process of using specific design constraints to achieve a design objective for a structure.

PHASE AVERAGE THEORY: A mathematical framework that relates the average stresses and strains in constituent phases to the overall composite response.

PLY: A single layer in a laminated composite material.

PREPREG: A reinforcing fabric or tape pre-impregnated with a polymer matrix, ready for layup and curing into composite laminates.

PSHELL (OPTISTRUCT): A shell property definition used in finite element models in Altair OptiStruct. It controls thickness, material linking, and formulation of shell behavior.

RESPONSES: In an optimization problem, responses are values measured from model changes such as stress.

REPRESENTATIVE VOLUME ELEMENT (RVE): The smallest volume of a heterogeneous material that can be considered statistically representative of its overall properties, used for homogenization.

SENSITIVITY ANALYSIS: A method to quantify how much variation in outputs can be attributed to different input variables.

STRAIN LIMIT (UNT0): The in-plane membrane strain output from Altair HyperView, used for validation and constraint checking in this study.

SURROGATE MODEL: A simplified mathematical approximation of a complex simulation, used to reduce computational cost during optimization.

UNIVERSAL TESTING MACHINE (UTM): A mechanical testing device used to apply controlled tension or compression loads while recording force and displacement.

WARP: The longitudinal direction in a woven lattice structure, typically aligned with the primary loading direction.

WEAV3D: A lattice weaving technology used to place thermoplastic tapes in orthogonal patterns, enabling tailored reinforcement in composite structures.

ACKNOWLEDGMENTS

I would like to express my sincere gratitude to Professor Marco Salviato for the opportunity to pursue this project under his supervision. As the chair of the committee, his leadership, guidance, and high standards played a central role in shaping the technical direction and overall quality of this work. His consistent support, both in research and throughout my time in the program, has been instrumental to my development as a graduate student. I am grateful for his thoughtful feedback, his deep understanding, and for pushing me to aim higher at every stage.

I am especially thankful to Jeff Wollschlager for being an outstanding mentor throughout this project. Jeff was involved at every level, from helping define the scope to building the computational framework, and providing invaluable technical and strategic input along the way. His ability to translate physical insight into practical modeling strategies was key to building the optimization workflow that underpins this thesis. More than that, his encouragement, patience, and generosity with his time made all the difference. Also, thank you for letting me use your lab!

I would also like to thank Dr. Peter Mackenzie-Helnwein and Dr. Avin Vijay for offering thoughtful guidance and mentorship. I am also grateful to everyone at MAMS for their feedback and input throughout the project.

Outside of academics, I would like to thank Paul Neubert and Betsy Winter for their help navigating the administrative and procedural side of graduate school, and for always being available when I needed support.

Finally, I want to thank my friends, family, and colleagues at the University of Washington for their constant encouragement and for being part of this journey.

Chapter 1

INTRODUCTION

Engineering materials continue to evolve as industries demand higher performance at lower weights and costs. While traditional fiber-reinforced composites offer excellent mechanical properties, their widespread adoption is hindered by high production costs and rigid design constraints. The Weav3D lattice structure technology called "Rebar for Plastics®" developed to address these limitations, represents an innovative approach to selective composite reinforcement. This concept creates woven patterns of thermoplastic prepreg tapes that can be embedded in structural components, providing targeted strength where needed most while reducing overall weight and cost. [61]

In this thesis, we will begin with material testing to obtain material properties and then we will implement the multiscale methodology for such lattice structures within an optimization framework to efficiently explore design possibilities. We will integrate the Jpanel software tool with Altair HyperStudy to systematically evaluate various design configurations. By parameterizing key design variables, we will demonstrate how to achieve optimized designs that balance performance requirements with weight and manufacturing constraints. Then, show that conventional optimization techniques work for these complex lattice structures.

1.1 Research Motivation

Traditional plastic reinforcement methods present significant limitations in automotive and aerospace applications. For decades, we have been accustomed to reinforced concrete in construction spheres and have tried to bring a similar methodology in other applications too. Some examples can include fiberglass reinforcement, metal inserts, sheet molding compound. All of these approaches have multiple shortcomings. For fiberglass reinforcements, they suffer from inconsistent fiber orientation, limited strength-to-weight efficiency, and

poor directional control [14]. Metal reinforcements add substantial weight and potential corrosion issues. These shortcomings result in over-engineered components, manufacturing inefficiencies, and unpredictable performance. The research into Weav3D lattice structure technology addresses these challenges by developing a systematic approach to analyze and optimize woven thermoplastic prepreg tape reinforcements. By creating a multiscale design methodology, we can accurately model these complex structures with reasonable computational efficiency, enabling precise control over reinforcement patterns and material usage. This work aims to provide a comprehensive framework for optimizing lightweight, high performance composite components that can outperform traditional reinforcement techniques in demanding applications.

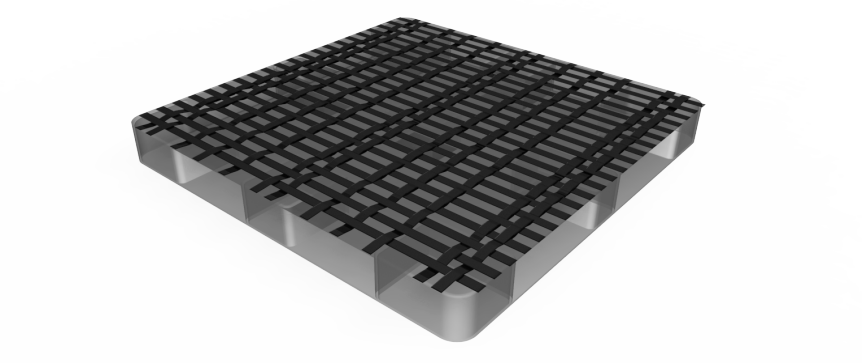

Figure 1.1: Visual rendering of a compression molded part reinforced with a Weav3D lattice. Demonstrates integration of reinforcement into molded geometry.[1]

1.2 Research Objectives and Scope

This work investigates whether conventional surrogate-based optimization strategies, commonly applied to monolithic and ply-based composites, are also valid and effective when used for architected thermoplastic lattice structures. These lattices, manufactured using the Weav3D process, consist of woven thermoplastic prepreg tapes embedded within molded plastic parts. The resulting architecture enables directional stiffness control by placing reinforcement only where it is structurally necessary, similar to rebar in concrete.

The primary objective of this study is to demonstrate that traditional design exploration

workflows, including Latin Hypercube Sampling (LHS), surrogate modeling, and Global Response Surface Method (GRSM) optimization, can be successfully applied to lattice-reinforced composites. Validating this methodology supports scalable, simulation-driven design of complex hybrid structures.

To avoid the computational burden of discrete modeling, this study uses an implicit multiscale approach. Lattice configurations are homogenized using the JPanel tool, which converts warp and fill tape definitions into orthotropic shell properties through MAT2 and PSHELL cards. This enables efficient parameter sweeps and optimization using Altair HyperStudy while preserving engineering-relevant accuracy.

The optimization framework focuses on minimizing structural mass while satisfying strain constraints in a three-point bending setup. Design variables include tape spacing, thickness, and material selection. The surrogate model is trained using over one hundred design points generated by Latin Hypercube Sampling and refined using Modified Extensible Lattice Sequence (MELS). Optimal configurations are selected through GRSM based on constraint satisfaction, surrogate prediction accuracy, and mass-strain trade-off quality.

For benchmarking purposes, a continuous quasi-unidirectional composite laminate is also analyzed. This allows for direct comparison between lattice-reinforced panels and traditional continuous layups under identical geometry and loading conditions.

(a) Thermoplastic Tape (b) Composite Lattice Layer (c) Molded Composite Lattice Part

Figure 1.2: Materials and structures used in lattice optimization framework [1]

1.3 Current State of Composite Lattice Modeling

The modeling and optimization of composite lattice structures represent an evolving field with several parallel approaches. Current methodologies can be broadly categorized into discrete modeling, simplified analytical methods, and emerging multiscale technologies.

Discrete modeling approaches, where each component of the lattice structure is explicitly represented in the finite element model, provide high fidelity but at significant computational cost. These models, while accurate, become time-consuming and computationally expensive for complex geometries and are impractical for design iterations and optimization studies.

Simplified analytical approaches[59] attempt to address this computational burden by representing lattice structures as equivalent homogeneous materials with effective properties. However, these methods often fail to capture the complex mechanical interactions between the reinforcement tapes and bulk material, particularly in bending load cases and thermal environments where the interactions are unique and different enough to not be captured through analytical means. [**?**]

Chapter 2

LITERATURE REVIEW & TECHNICAL BACKGROUND

The design and analysis of composite lattice structures require a foundational understanding of both the physical materials involved and the theoretical principles that govern their behavior. This chapter provides the essential background knowledge needed to comprehend the multiscale modeling approach and the problem we are faced with. We begin by examining the unique nature of Weav3D lattice structures and their manufacturing process, which creates distinctive challenges compared to traditional composite laminates. We then explore the theoretical frameworks that enable the efficient modeling of these systems, including homogenization techniques, phase average theory, and modified classical lamination theory.

The background presented here establishes the basis for the novel methodology proposed in subsequent chapters, highlighting both the limitations of current approaches and the opportunities for advancement. By understanding these fundamental concepts, we can appreciate the significance of developing a computationally efficient yet accurate modeling framework that can capture the complex mechanical behavior of composite lattice structures while facilitating practical design optimization.

2.1 Manufacturing process of Weav3D lattice structures

The manufacturing process of Weav3D lattice structures involves a sophisticated approach to create thermoplastic composite reinforcements. The process begins with thermoplastic prepreg tapes that are woven into controlled geometry. These lattices can be customized by varying parameters such as tape material (carbon, glass, or other fibers), tape width, tape gap spacing, and the number of lattice layers. [61]

The manufacturing process involves laying down unidirectional tapes in warp and fill (weft) directions to create the desired pattern, followed by a consolidation step. The tapes

are first cut to length and then precisely placed adjacent to each other without overlapping. They are then tack-welded at multiple spots using an ultrasonic welder (Dukane IQ-HP-E 30K 600W with Hand Probe) to hold them in position. For additional layers, the tapes may be offset by half a tape width or arranged according to a specific pattern. The assembled lattice is then heat pressed at approximately 185°C for about 2 minutes and subsequently transferred to a hydraulic press for consolidation under pressure (usually 7000 lbf for 1 minute). Once consolidated, these lattice structures can be embedded in thermoplastic structural components through injection or compression molding processes, creating "Rebar for Plastics" that combines the performance benefits of continuous fiber reinforcement with the cost advantages and ease of production associated with discontinuous fiber reinforced plastics. [42]

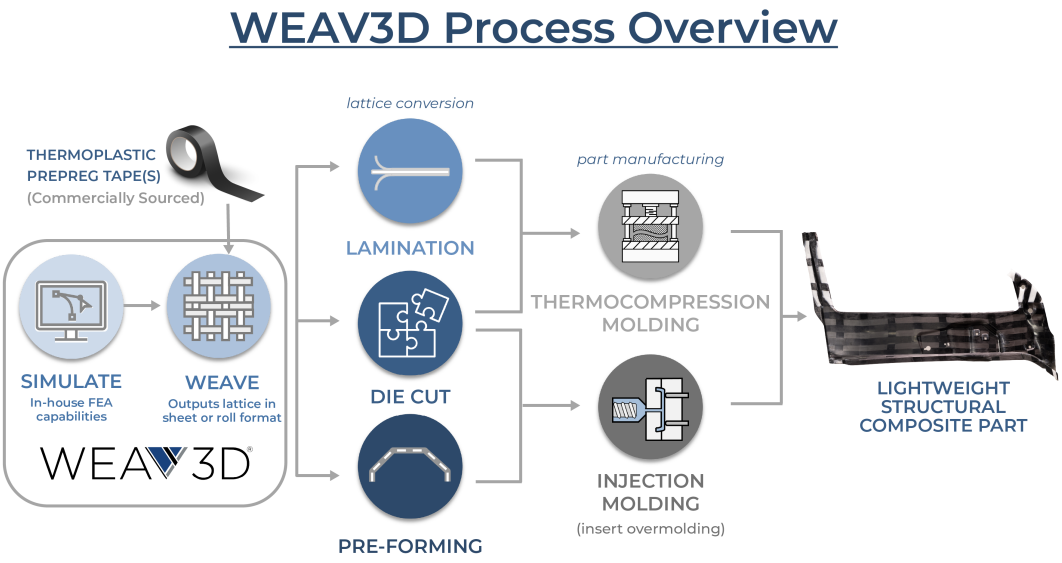

Figure 2.1: The Weav3D automated lattice weaving system [4]

2.2 Design and Analysis Challenges

Traditional finite element analysis techniques developed for isotropic materials or standard-ply based composites fail to capture the complex physical properties and material behavior

of these heterogeneous structures. The design space becomes exponentially complex when considering the numerous variables that define a lattice structure. This complexity is further magnified when variable tape densities and different material types coexist within a single layer. While discrete modeling explicitly representing each tape element can provide accurate results, it becomes time-consuming and computationally expensive for applications [23].

Moreover, the multiscale nature of these structures introduces additional modeling challenges, as local stress concentrations below the scale of the repeating volume unit cannot be adequately resolved with conventional approaches. These limitations require a more sophisticated modeling methodology, setting the stage for multiscale approaches that can effectively bridge the gap between microscale material behavior and macroscale structural performance.

2.3 Multiscale Modeling Approach

The multiscale modeling approach represents a fundamental shift in analyzing Weav3D lattice structures by connecting material behavior at different scales. This methodology combines Phase Average Theory and Classical Lamination Theory to create a framework specifically tailored for lattice-reinforced composites.[61]

The approach works at two connected scales: homogenization, where the complex geometry of lattice layers is transformed into equivalent material properties, and dehomogenization, where overall structural responses are translated back to local tape and matrix behaviors. By developing representative volume elements (RVEs) that capture the essential characteristics of the lattice structure, engineers can model the effective properties without having to represent every tape in detail.

This method assumes that the RVE repeats uniformly throughout a region, with its properties characterizing the entire area. The mathematical formulation accounts for volume fractions of different materials, their respective properties, and geometric configurations, ensuring that both flat and bending behaviors are accurately represented.

Although currently optimized for linear elastic analysis, the framework maintains good engineering accuracy, typically within 15% of detailed modeling results, all while dramat-

ically reducing modeling complexity and computational demands. The real advantage of this approach is its ability to facilitate rapid design iteration, allowing engineers to explore many design options without the time constraints of traditional modeling techniques. This efficiency transforms a difficult analysis challenge into a practical design opportunity.

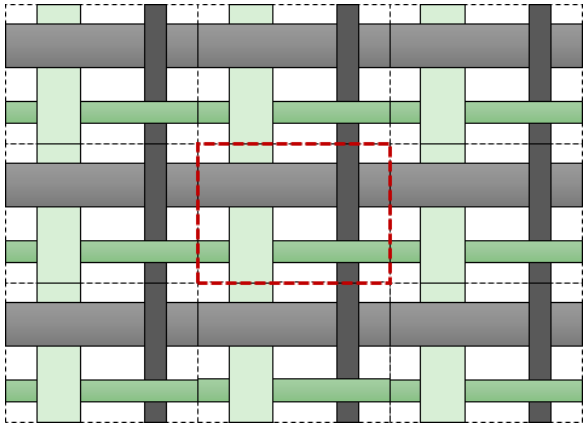

Figure 2.2: Lattice Repeating Unit Volume (Implicit Design Methodology) [61]

2.4 Manufacturability Assessment of Optimized Lattice Designs

While the preceding sections detail the optimization of lattice-reinforced composite panels using multiscale FEA workflows, it is equally important to evaluate the manufacturability of the optimized designs. Unlike traditional continuous fiber composites, where cost and fabrication complexity are major bottlenecks, the Weav3D process offers a scalable, cost-effective alternative by leveraging woven thermoplastic lattice reinforcements, branded as "Rebar for Plastics®".

The lattice used in this study is fundamentally compatible with the Weav3D process. It is manufactured from commercially available thermoplastic prepreg tapes (typically 1 inch in width), woven and consolidated using Weav3D's automated forming machine. The standard process supports high-throughput production via integration with existing injection or compression molding equipment, enabling part cycle times in the range of 2–5 minutes.

Critically, the process supports variable lattice density which is a core feature of the optimization framework developed in this thesis. Regions of the part that require less stiff-

ness can be reinforced with lower density lattices, reducing both material cost and trim waste. This feature aligns directly with the parameterization strategy used in HyperStudy, where tape gap and lattice spacing are actively varied to minimize mass while maintaining structural performance.

One consideration is that the minimum lattice spacing is bounded by the physical tolerances of the Weav3D weaving system and tape consolidation process. While the standard 25 mm tape was assumed in this work, future extensions of the optimization may include constraints to ensure realistic tape overlap and spacing within manufacturable limits. Nonetheless, all optimized configurations developed in this study are expected to fall within feasible manufacturing windows, provided that the final lattice geometry respects minimum tape width, gap spacing, and fiber orientation constraints as supported by the Weav3D weaving platform.

These diverse manufacturing options allow Weav3D to serve both low- and high-volume production markets across automotive and aerospace applications. By integrating directly into common molding workflows such as D-LFT compression forming and injection overmolding, the technology bridges the gap between simulation-driven composite design and scalable, cost-effective part fabrication. The ability to vary lattice density in localized regions further enhances this compatibility, enabling tailored performance without custom tooling or layup strategies.

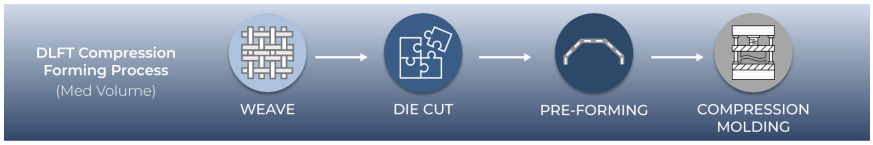

(a) D-LFT Compression Molding

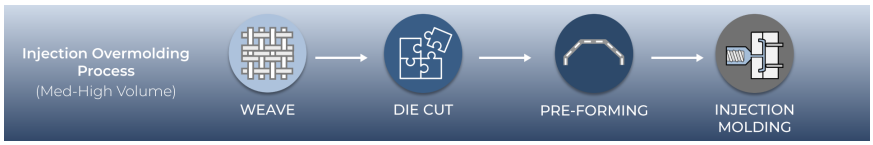

(b) Injection Overmolding

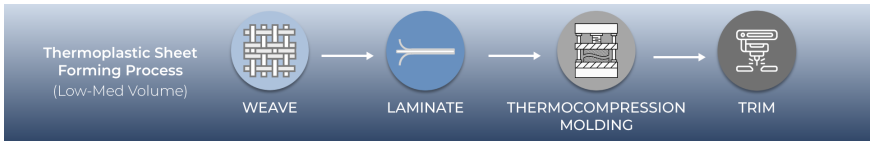

(c) Thermoplastic Sheet Forming

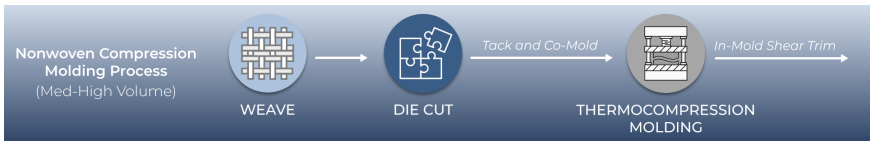

(d) Nonwoven Molding Integration

Figure 2.3: Overview of four Weav3D-compatible composite manufacturing processes. Each enables integration of lattice reinforcements into standard thermoplastic workflows with minimal tooling changes. [4]

2.5 Material System Capabilities and Hybrid Reinforcement

Building on the previous sections, one critical question remains: Why this approach? How can we justify that the proposed design methodology offers the most practical and effective solution? To address this, it is essential to highlight the inherent material and process versatility of the Weav3D platform.

As shown in the figure below, the Weav3D process supports a wide range of commercially

available thermoplastic prepreg tapes, enabling reinforcement customization tailored to specific cost, strength, and processing requirements. Material combinations include low-cost glass/PP tapes for economical stiffness, mid-range carbon/PA6 for balanced mechanical and thermal performance, and high-performance carbon/PEEK systems for aerospace-grade applications. Matrix compatibility spans a broad spectrum from common polymers such as PP and PA6 to advanced formulations including PAEK, PEEK, and select thermosets like unsaturated polyester and vinyl ester.

This materials flexibility enables seamless integration into multiple molding workflows, including injection molding, compression molding, thermoforming, and even nontraditional domains like polymer concrete. Furthermore, the continuous fiber lattice reinforcement can be combined with short or long glass-filled thermoplastic compounds (e.g., SMC, BMC, or D-LFT), forming a hybrid reinforcement system. This structure operates across multiple length scales, enabling targeted tuning of mechanical properties such as stiffness, strength, and impact resistance either globally or within localized regions of the part. As a result, the Weav3D framework supports both structural optimization and manufacturing efficiency, minimizing the need for excessive reinforcement while meeting or exceeding performance targets. [1]

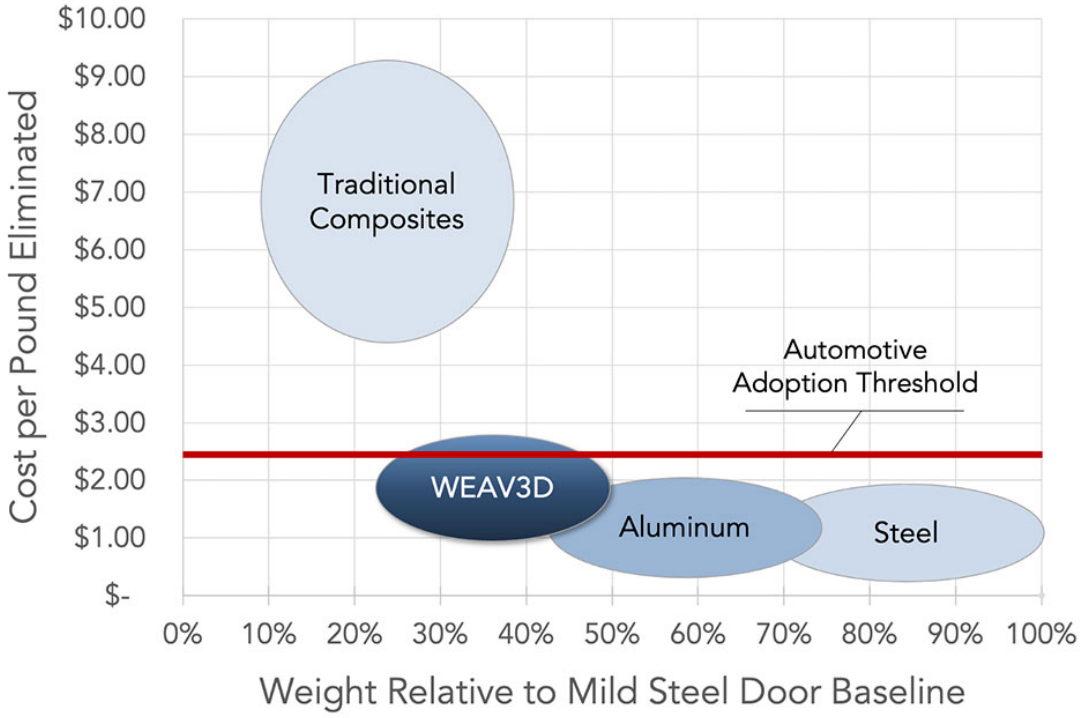

Figure 2.4: Cost-to-weight tradeoff of Weav3D vs. conventional materials. The Weav3D system falls below the automotive adoption cost threshold, offering competitive structural efficiency relative to aluminum and steel. [1]

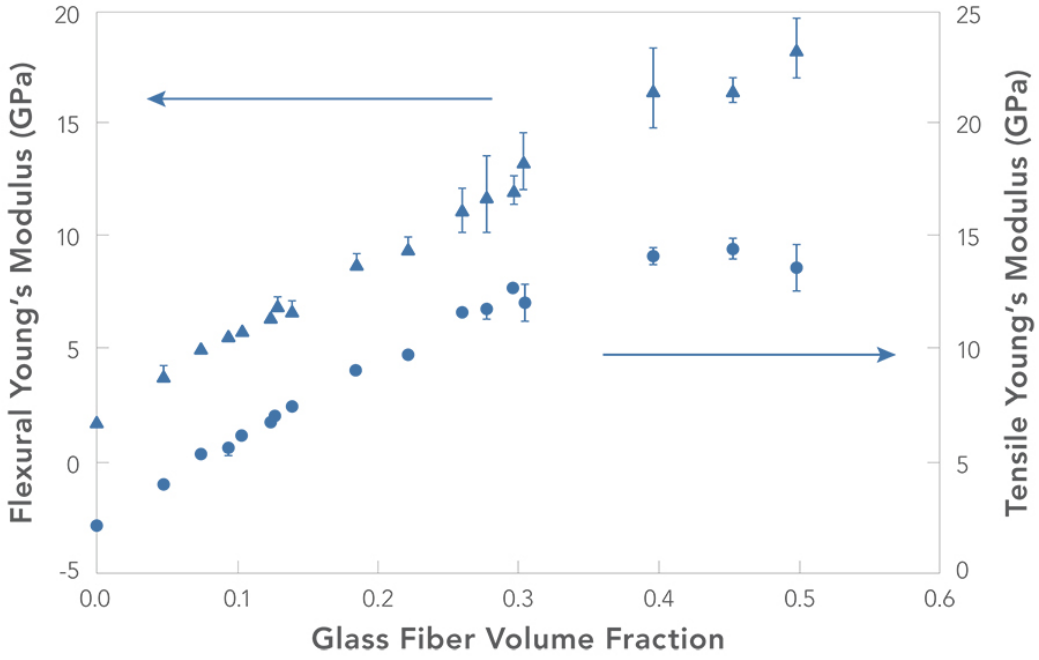

Figure 2.5: Flexural and tensile Young's modulus of glass-filled thermoplastics as a function of glass fiber volume fraction. This illustrates the stiffness improvement potential of hybrid composite systems using discontinuous glass fiber reinforcement. [1]

Table 2.1: Representative fiber–matrix systems compatible with the Weav3D lattice reinforcement process. Thermoset configurations such as vinyl ester may support variable fiber types depending on structural and processing requirements.

Fiber	**Matrix**	**Application Tier**	**Notes**
Glass	PP	Automotive	Low cost, injection molded
Carbon	PA6	General purpose	Good strength, thermoplastic compatibility
Carbon	PEEK	Aerospace	High temp, excellent stiffness
Glass/Carbon	Vinyl Ester	Thermoset Panel	Pultrusion-compatible; fiber choice varies

Table 2.1 summarizes the core material systems currently supported by the Weav3D [4], showing a balance between low-cost, general-purpose, and high-performance configurations across both thermoplastic and thermoset applications.

The breadth of compatible fiber–matrix systems highlights the versatility of the Weav3D platform across a range of structural applications. Whether targeting low-cost automotive components or high-performance aerospace parts, the process supports tailored reinforcement strategies without compromising manufacturability. This material flexibility further strengthens the case for lattice-based optimization as a scalable and application-agnostic design methodology.

The Weav3D process enables thermoplastic prepreg tapes to be interlaced into customizable lattice patterns before being embedded into a structural laminate. This architecture allows for directional tailoring of stiffness and strength while minimizing unnecessary reinforcement in low-strain regions. The flexibility of the weaving process also introduces

multiple design parameters, such as warp and fill spacing, tape width, and the number of lattice layers. Exploring this large design space using full-scale finite element models is computationally intensive, making a direct optimization approach impractical for this work.

2.6 Surrogate-Based Optimization Approach

The complex geometry and directional stiffness tailoring possible with the Weav3D process introduce a wide range of design variables, making direct optimization using high-fidelity finite element analysis computationally impractical. While gradient-based optimization methods can be efficient when derivative information is available, they become computationally expensive for problems requiring high-fidelity simulations. Laurenceau and Allen [34] compared gradient-based frameworks with surrogate-based approaches and found that surrogates can achieve similar performance with significantly fewer simulation evaluations. Queipo et al. [53] provided a comprehensive review of surrogate modeling techniques such as kriging and response surfaces, highlighting their suitability for nonlinear and computationally intensive design problems. These studies support the use of surrogate-based optimization in this work, where each finite element simulation carries a high computational cost.

Following this methodology, the next stage involves accurately characterizing the material properties of the lattice-reinforced laminates to ensure that the surrogate model is informed by realistic input data. This is achieved through digital image correlation (DIC) testing on coupon specimens, as described in the subsequent section.

Chapter 3

DESIGN AND OPTIMIZATION FRAMEWORK SETUP

This chapter presents the framework developed for optimizing Weav3D lattice structures in thermoplastic components using Altair HyperStudy. The approach combines experimental material characterization with a multiscale modeling strategy to connect microscale properties to macroscale structural performance. By incorporating measured material properties into the optimization workflow, the methodology ensures that simulation results reflect realistic behavior rather than relying solely on nominal datasheet values.

The optimization challenges posed by these complex woven architectures are addressed through a phase-averaged, modified classical lamination theory. This mathematical foundation enables the detailed geometry of the woven tapes to be represented by homogenized properties that retain sufficient accuracy for design evaluation while avoiding the computational cost of fully discretizing every tape and gap in the finite element model.

The chapter begins with the experimental characterization of carbon fiber thermoplastic tapes using digital image correlation (DIC) to determine the in-plane moduli, shear stiffness, and Poisson's ratios. These results form the basis for defining the baseline panel configuration and lattice-reinforced variants. The subsequent sections describe how these properties are integrated into the homogenization process via JPanel, how the baseline and lattice finite element models are constructed in HyperMesh, and how HyperStudy is used to conduct the design of experiments (DOE) [7] and optimization studies.

3.1 Experimental Characterization of Carbon Fiber Tapes

To accurately characterize the mechanical properties of the carbon fiber tapes used in this study, a series of physical tests were conducted using Digital Image Correlation (DIC) in conjunction with a Universal Testing Machine (UTM). These experiments were designed to extract the orthotropic elastic properties, namely, longitudinal modulus ($E1$), trans-

verse modulus ($E2$), and in-plane shear modulus ($G12$) that form the foundation of the MAT9OR material models used in the optimization framework. The experimentally obtained data enable direct validation of the material behavior assumed in the homogenized lattice simulations. Although these tests were conducted after the optimization was initially developed, they serve as the true starting point for any multiscale simulation effort involving architected materials such as Weav3D lattices.

3.1.1 Test Setup and Procedure

All material property tests were performed using DIC [40] with full-field strain measurement. A MatchID system was used for DIC capture and processing, paired with an electromechanical UTM equipped with a standard load cell (model specifications noted in Appendix X). The data acquisition rate was set at 5 Hz. Both virtual and real extensometers were placed in 2 separate tests to make sure data did not skew to one side.

Carbon fiber tapes were tested in the raw form as straight, untabbed coupons. To enable accurate strain capture, a high-resolution speckle pattern was applied using the water-transfer tattoo paper method. The process involved printing a speckle pattern on standard A4 tattoo transfer sheets using a high-resolution printer. Once printed, a laminate layer was applied over the sheet, which was later peeled to expose the adhesive speckle surface. Strips were cut from the speckle sheet and adhered to the surface of the carbon tapes after surface cleaning with 91% isopropyl alcohol. The adhesive speckle strip was positioned along the tape gauge section, wetted slightly with water to activate the backing layer, and the paper carrier was removed, leaving the speckle layer fixed on the tape. The samples were allowed to dry overnight before being loaded into the UTM grips for testing.

Each specimen was tested under specific loading configurations: longitudinal tension (LT), transverse tension [2], and in-plane shear [3]. These configurations allowed for the isolation of the respective elastic constants and were repeated twice per loading mode to ensure statistical consistency. For each test, approximately 16 images were captured before the onset of deformation. These images were averaged and used as the reference condition within MatchID. A final image captured just prior to complete fracture was selected as the

deformed state. Strain fields were calculated based on this image pair, providing full-field strain maps used to evaluate elastic behavior.

All graphing, slope extraction, and numerical computations were carried out manually in Microsoft Excel using the extensometer-based strain data exported from MatchID. Each configuration was tested at least twice, and the final elastic constants were computed as simple averages across repeated runs.

3.1.2 Longitudinal Tension (LT) – Extraction of E1

The longitudinal tension (LT) test is performed to extract the axial modulus $E1$ of the carbon fiber-reinforced thermoplastic tape, corresponding to the fiber-aligned direction (0°). Under Classical Laminate Theory (CLT), this direction primarily governs the in-plane stiffness of unidirectional composites, making it a critical property for accurate simulation and optimization of warp-dominated lattice structures.

In this configuration, the carbon fiber tows are oriented along the loading axis. Tensile loading is applied uniaxially, and the DIC system captures full-field strain distributions along the gauge section. As the reinforcement fibers dominate the mechanical response in this direction, the measured strain–stress behavior provides a direct evaluation of $E1$. Two LT samples were tested and strain data was captured.

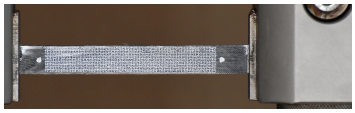

(a) Test 1 - Image A (Reference)

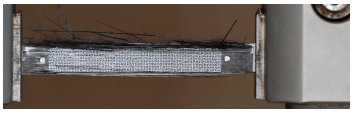

(b) Test 1 - Image B (Pre-deformation)

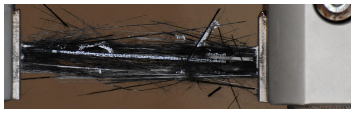

(c) Test 1 - Image C (Deformed)

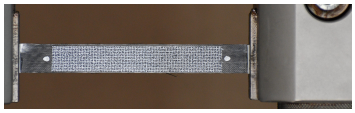

(d) Test 2 - Image A (Reference)

(e) Test 2 - Image B (Pre-deformation)

(f) Test 2 - Image C (Deformed)

Figure 3.1: Digital image correlation (DIC) snapshots of carbon fiber tapes during longitudinal tension (LT) testing. Each row shows reference, pre-deformation, and deformed images for a single test.

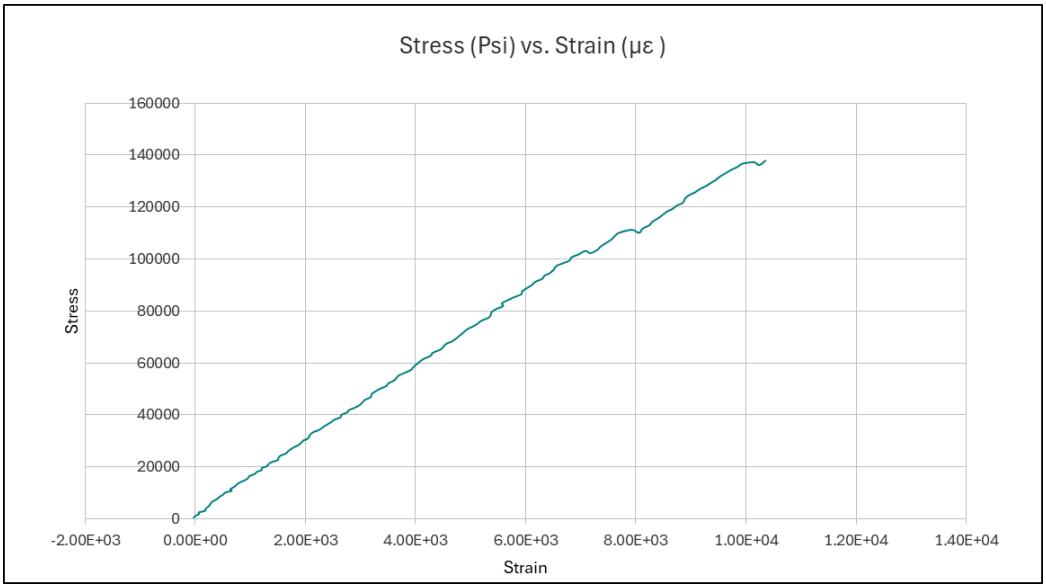

Figure 3.2: Stress-strain curve. The X-axis represents strain ($\mu\varepsilon$) and the Y-axis represents stress (psi).

From the graph above, the slope was calculated to be $E1 = 94500$ MPa or 94.5 GPa.

3.1.3 Transverse Tension (TT) – Extraction of E_2

The transverse tension (TT) test is conducted to extract the transverse modulus E_2 of the carbon fiber-reinforced thermoplastic tape, corresponding to the matrix-dominated direction (90°). In Classical Laminate Theory (CLT), this property reflects the composite's stiffness response perpendicular to the fiber direction and is primarily governed by the resin matrix, with some minor influence from fiber misalignment and interfacial bonding.

In this configuration, the carbon fiber tows are oriented perpendicular to the loading axis. Since the matrix primarily carries the load in this direction, the resulting strain–stress relationship captures the bulk resin response under tension and is critical for capturing through-thickness and off-axis response in laminate or homogenized lattice simulations.

Two TT samples were tested using the same DIC setup as LT. The speckle pattern was applied using the tattoo paper transfer method, and 16 reference images were averaged to generate the undeformed base image. Final deformed images were captured just prior to failure for each sample.

Strain data was extracted using virtual extensometers aligned with the loading direction, and stress was computed based on known cross-sectional area and applied load from the UTM. From these, E_2 was calculated as the slope of the linear elastic portion of the stress–strain curves. The final transverse modulus was obtained by averaging the results from both TT tests.

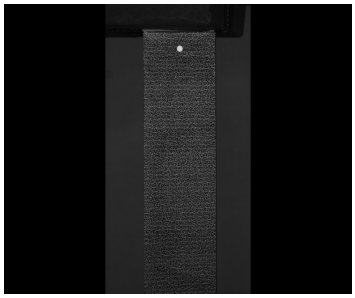

(a) Test 1 - Image A (Reference)

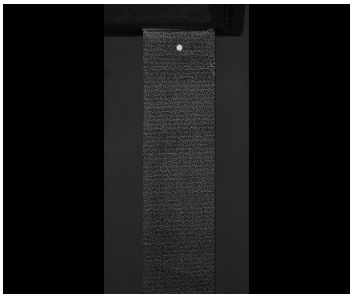

(b) Test 1 - Image B (Pre-deformation)

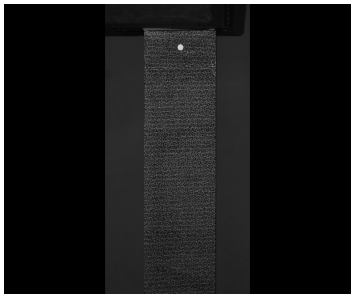

(c) Test 1 - Image C (Deformed)

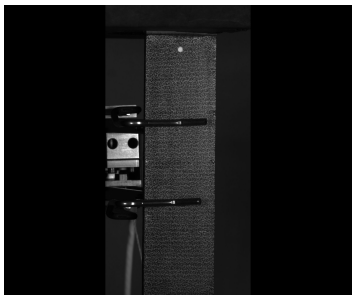

(d) Test 2 - Image A (Reference)

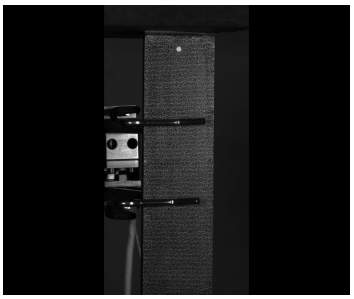

(e) Test 2 - Image B (Pre-deformation)

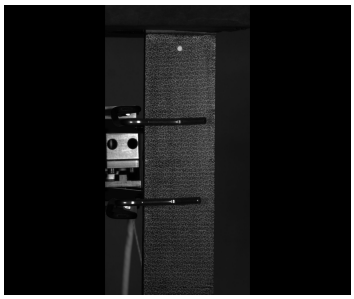

(f) Test 2 - Image C (Deformed)

Figure 3.3: Digital image correlation (DIC) snapshots of carbon fiber tapes during transverse tension (TT) testing. Each row shows reference, pre-deformation, and deformed images for a single test.

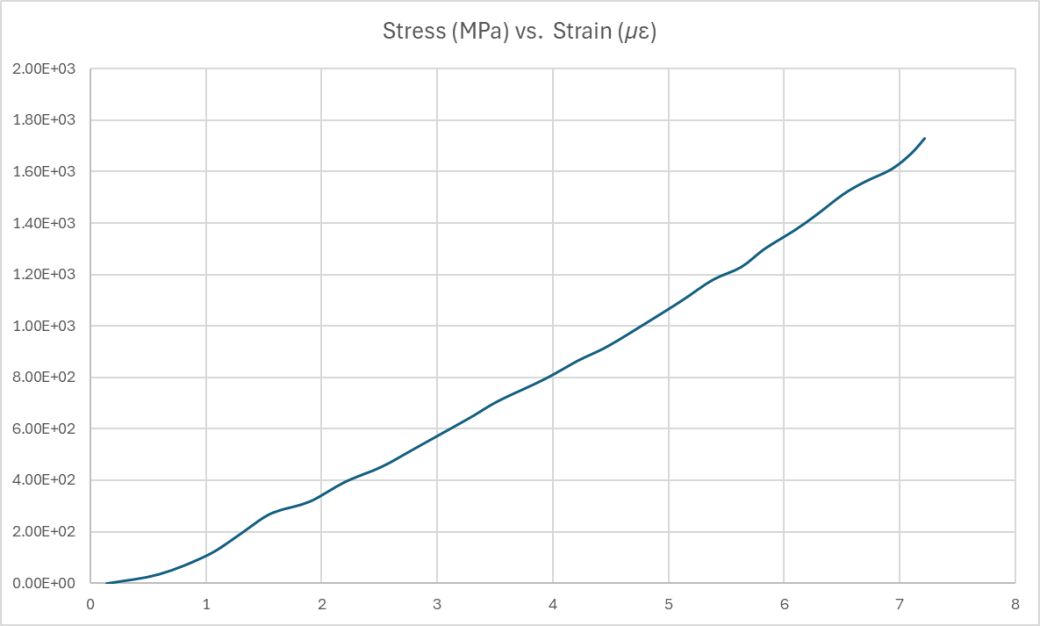

Figure 3.4: Stress-strain curve. The X-axis represents stress (MPa) and the Y-axis represents strain ($\mu\varepsilon$).

From the graph above, the slope was calculated to be $E2 = 4200$ MPa or 4.2 GPa.

3.1.4 In-Plane Shear (IPS) – Extraction of G_{12}

The in-plane shear (IPS) test was conducted to extract the shear modulus G_{12} of the carbon fiber tape, which characterizes the material's stiffness under shear loading within the fiber–matrix plane. This parameter is fundamental in Classical Laminate Theory (CLT), especially for predicting off-axis deformation and assessing the response of composite laminates under general loading conditions.

To promote a pure in-plane shear condition, specimens were cut and loaded in a $\pm 45^\circ$ orientation relative to the fiber axis. When subjected to axial tension, this configuration induces a uniform shear state across the gauge region. Full-field shear strain was captured using Digital Image Correlation (DIC) and processed using the MatchID software suite.

Unlike tension tests, IPS loading was not carried out to failure. Since $\pm 45^\circ$ specimens typically undergo large deformations before rupture, testing was limited to the linear regime.

The goal was to obtain an accurate measure of G_{12} from the slope of the initial linear portion of the stress–strain response.

Two IPS specimens were tested, and results were averaged to improve accuracy. The resulting shear modulus served as input to the MAT9OR definition of the carbon fiber material used in the homogenized simulation model.

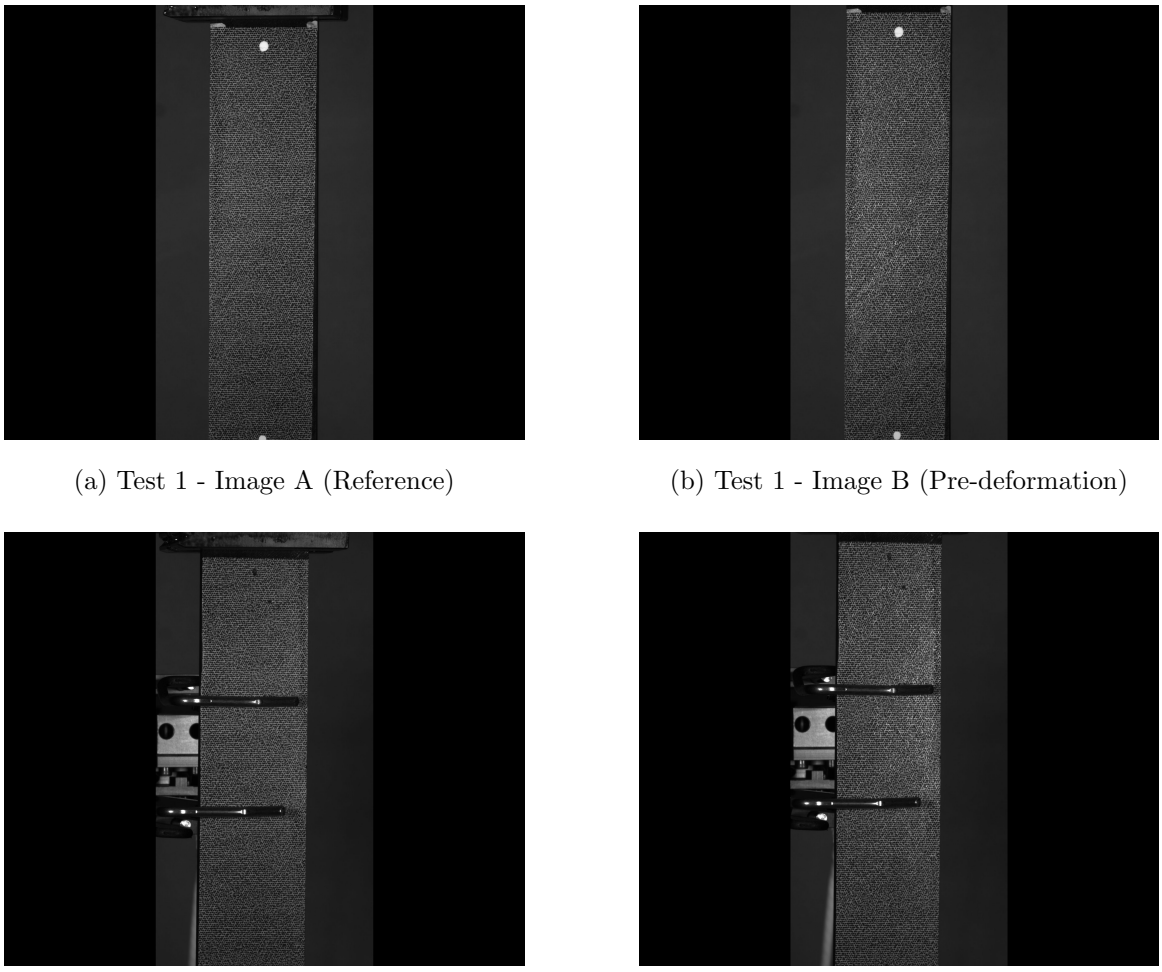

(a) Test 1 - Image A (Reference)

(b) Test 1 - Image B (Pre-deformation)

(c) Test 2 - Image A (Reference)

(d) Test 2 - Image B (Pre-deformation)

Figure 3.5: Digital image correlation (DIC) snapshots of carbon fiber tapes during in-plane shear (IPS) testing using $\pm 45^{\circ}$ specimens.

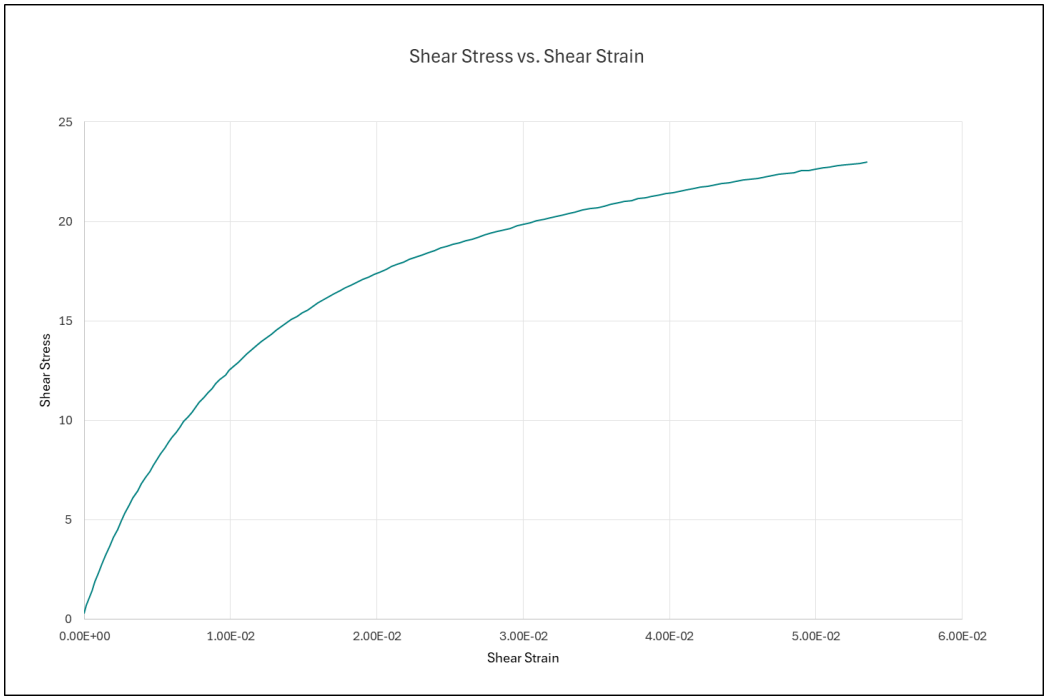

Figure 3.6: Shear stress-strain curve. The X-axis represents shear strain ($\mu\varepsilon$) and the Y-axis represents shear stress (MPa).

From the graph above, the slope was calculated to be $G12 = 1300$ MPa or 1.3 GPa.

3.1.5 Validation of DIC-Derived E_1 Using Membrane Strain Output (UNT0)

To validate the accuracy of the axial modulus obtained from digital image correlation (DIC), the membrane strain result labeled as `UNT0` was compared against a theoretical stiffness estimate derived from Classical Laminate Theory (CLT). An in-house Excel model was used to compute the effective in-plane modulus E_x of an 8-ply laminate, based on the experimentally extracted values for E_1, E_2, G_{12}, and G_{23}.

The laminate model yielded an E_x of 4.9956×10^4 MPa, while the DIC-derived `UNT0` value was measured as 49871.54 MPa. This represents an error of less than 0.26%, confirming that the mechanical behavior predicted by the DIC setup closely aligns with analytical expectations. This validation provides confidence in the reliability of the extracted moduli

for downstream simulation and optimization.

The validated material properties extracted through DIC testing including E_1, E_2, G_{12}, and G_{23} serve as the foundational inputs for all subsequent stages of this study. These experimentally derived parameters are directly integrated into the Jpanel homogenization process, more specifically, in the MAT9OR* material card and utilized throughout the design exploration, surrogate modeling, and optimization workflow. By anchoring the simulation framework in physical testing, the resulting lattice optimization is grounded in accurate, measurable behavior of the carbon fiber composite tape system.

Table 3.1: Extracted Orthotropic Properties for Carbon Composite (MAT9OR)

Parameter	**Value**	**Description**
E_1	94.5 GPa	Longitudinal Young's modulus
E_2	4.2 GPa	Transverse Young's modulus (in-plane)
ν_{12}	0.35	Major Poisson's ratio (1-2 plane)
ν_{23}	0.0156	Poisson's ratio (2-3 plane)
G_{12}	1.3 GPa	Shear modulus in 1-2 plane
G_{23}	2.84 GPa	Shear modulus in 2-3 plane

3.2 Geometry and Composite Layout

The panel used in this study serves as the baseline geometry for all simulations and optimization runs. It is a flat composite laminate reinforced with a woven lattice and sized to represent a three-point bending test configuration. The dimensions, reinforcement layout, and coordinate conventions are defined here to establish a consistent reference for all subsequent models.

3.2.1 Panel Dimensions and Setup

The panel has the following dimensions (consistent with prior work by Wollschlager [61]):

- **Length (X direction)**: 177.8 mm
- **Width (Y direction)**: 127.0 mm
- **Total nominal thickness (Z direction)**: 2.54 mm (0.25 in)

The coordinate system is defined such that:

- The **X-axis** runs along the length of the panel and is aligned with the primary bending load.
- The **Y-axis** runs across the width of the panel.
- The **Z-axis** is the through-thickness direction, normal to the panel surface.

3.2.2 Reinforcement Orientation and Terminology

The embedded lattice consists of woven thermoplastic prepreg tapes arranged in two orthogonal families:

- **Warp direction**: aligned with the X-axis (lengthwise), parallel to the direction of bending.
- **Fill direction**: aligned with the Y-axis (widthwise), orthogonal to the warp.

Tapes may be placed on either the **top** or **bottom surfaces** of the panel, and the model permits asymmetric layering. Each direction (warp and fill) can be independently varied in terms of tape spacing, tape width, tape thickness, and number of layers.

The following directional identifiers are used throughout this study:

- **W1** = Warp tape on bottom surface
- **W2** = Warp tape on top surface
- **F1** = Fill tape on bottom surface

- **F2** = Fill tape on top surface

This naming convention is consistently applied across simulation setup, parameter files, and response monitoring. For example, a strain measurement labeled `LW1B` refers to Lattice Warp 1 (bottom surface).

3.2.3 Shell Midplane Modeling

All panels are modeled using shell elements, with material properties applied at the midplane. The reinforcement configuration is homogenized and assigned using orthotropic MAT2 and PSHELL cards. This approach captures both in-plane and bending behavior of the lattice-reinforced composite while avoiding the complexity of discrete tape modeling.

3.3 Optimization Workflow Implementation

This section describes the full modeling and optimization workflow used in this study. The framework integrates the multiscale homogenization tool `Jpanel` with Altair's `HyperStudy` software to enable surrogate-based optimization of lattice-reinforced composite structures.

The overall goal is to explore how varying the spatial layout and material selection of a Weav3D lattice influences structural mass and strain performance under three-point bending and whether conventional optimization strategies apply for tailored lattice structures.

A baseline model using a continuous composite panel with quasi-unidirectional plies was constructed. This model was generated by modifying the `Jpanel` input to simulate uniform stiffness without lattice architecture, enabling a full optimization workflow.

3.3.1 Parameter Definition and Design Variables

The design space includes both geometric and material parameters that control the reinforcement layout of the panel. The variables are listed below:

- **Tape gap spacing (GAP W, GAP F)**: Center-to-center distance between adjacent warp or fill tapes, measured along the panel surface.

- **Tape width (WTH W1, WTH W2, WTH F1, WTH F2)**: Width of the individual tapes in each direction and layer.
- **Tape thickness (THK W1, THK W2, THK F1, THK F2)**: Thickness of each tape, which contributes to panel height and bending stiffness.
- **Number of lattice layers (NUM L)**: Total number of warp-fill lattice layers stacked in the through-thickness direction.
- **Tape and bulk material types**: Material choices for the tapes (e.g., carbon/PP, glass/PA6) and the surrounding thermoplastic matrix.

To reduce dimensionality and maintain consistency with manufacturing capabilities, some parameters were held constant throughout the study. In particular, tape width and thickness were fixed at standard values based on commercially available tape formats. The table below summarizes the variable configuration.

Table 3.2: Design Variables and Parameter Roles

Variable	**Description**	**Unit**	**Status**
GAP W	Warp tape spacing	mm	Variable
GAP F	Fill tape spacing	mm	Variable
WTH W1/W2	Warp tape width (top/bottom)	mm	Fixed
WTH F1/F2	Fill tape width (top/bottom)	mm	Fixed
THK T	Tape thickness	mm	Fixed
NUM L	Number of lattice layers	Integer	Fixed
Material	Tape and bulk material type	N/A	Variable

All variable bounds were chosen to balance physical feasibility with computational tractability. For example, minimum tape spacing was limited to avoid tape overlap, while maximum spacing was constrained to ensure sufficient reinforcement coverage.

3.3.2 Two-Step Simulation and Optimization Framework

The optimization system is built around a two-step process implemented in HyperStudy. This dual-step structure automates the simulation pipeline and enables the evaluation of dozens to hundreds of design candidates with minimal manual effort.

Step 1: Material Homogenization via `Jpanel`

In the first loop, HyperStudy writes a parameterized `.fem` file based on the current design input. This file is passed to `Jpanel`, which performs homogenization of the input lattice geometry. The output is a `MAT2` and `PSHELL` include file that encapsulates the orthotropic stiffness, density, and directional properties of the reinforced panel.

Step 2: Finite Element Analysis via HyperMesh and OptiStruct

The homogenized include file is inserted into a generic shell panel model using HyperMesh. The model is then solved using OptiStruct to evaluate displacement and mass. Output quantities are extracted and returned to HyperStudy, which logs the results and proceeds to the next design iteration.

3.3.3 Role of HyperStudy

HyperStudy functions as the central control system for managing input-output connections, parameter updates, and optimization logic. It enables:

- Automated variation of design parameters using sampling or optimization algorithms.
- Management of dependencies between input templates and generated simulation files.
- Collection and storage of simulation results including displacements, mass, and strain fields.
- Integration with surrogate modeling and optimization routines for efficient exploration.

In this framework, HyperStudy does not evaluate gradients or internal physics directly. Instead, it coordinates the execution of `Jpanel` and `OptiStruct` to perform high-fidelity simulations at each design point.

3.3.4 Template File Integration

A key feature enabling automation is the use of template files. The master input file contains placeholder tokens (e.g., `#GAP_W#`) that HyperStudy replaces with actual values during each run. This system enables:

- Efficient parameter substitution without user intervention.
- Seamless integration of lattice parameters into `Jpanel` and shell modeling tools.
- Scalable batch simulation across hundreds of design variants.

The use of templates ensures that each design iteration is traceable and reproducible, with a clearly defined input-output mapping.

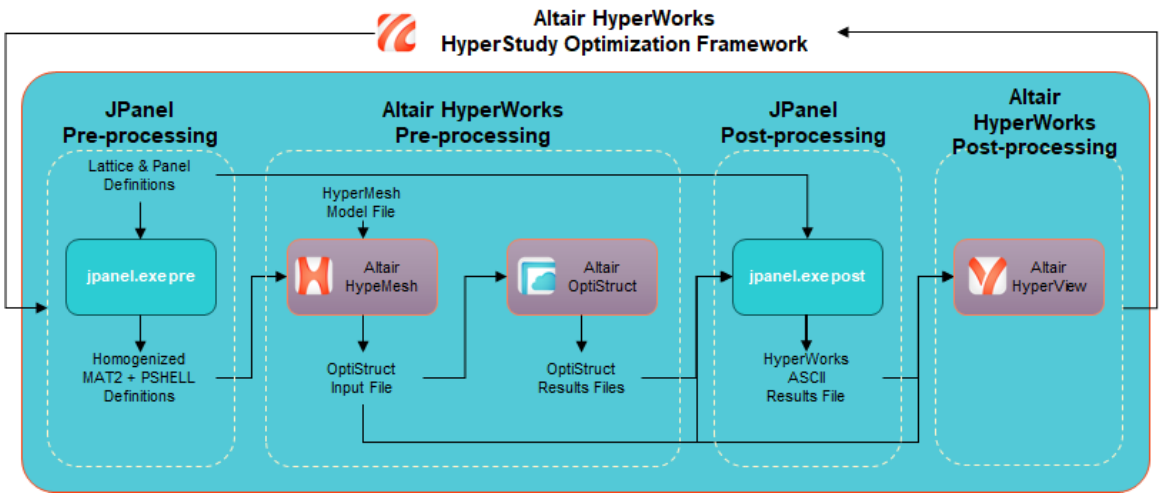

Figure 3.7: HyperStudy Framework

3.4 Material Model and Implicit Shell Representation

In order to efficiently simulate the mechanical response of lattice-reinforced composite structures, an implicit modeling approach was adopted. Rather than modeling each individual tape and ply discretely within the finite element mesh, the panel is treated as a homogenized

orthotropic shell. This enables simulation of complex reinforcement architectures with a reduced element count and faster solve times, while still capturing directionally dependent stiffness and mass behavior.

3.4.1 Implicit Modeling Strategy

Implicit modeling refers to the representation of a complex internal geometry such as warp and fill tape networks using averaged or homogenized material properties, without explicitly resolving the physical features in the mesh. In this study, the tapes are not individually meshed or modeled as solid volumes. Instead, their structural contribution is captured through an equivalent orthotropic material definition applied to shell elements.

This approach is particularly well-suited to optimization studies where multiple design variations are analyzed. Modeling each design with discrete tows would be computationally intractable, especially given the number of DOE and optimization samples used. By contrast, the implicit model allows fast evaluations of dozens to hundreds of design points while preserving sufficient fidelity to capture bending, membrane, and shear behavior.

3.4.2 MAT2 and PSHELL Definitions

The finite element model uses second-order shell elements with material properties assigned using a combination of `MAT2`[8] and `PSHELL`[9] entries. These definitions are generated automatically by `Jpanel` based on the lattice configuration for each design point.

- `MAT2` defines a linear elastic plane stress anisotropic material stiffness matrix [Q].
- `PSHELL` assigns the shell thickness and links the material definition to the mesh. It also defines the bending and membrane behavior based on the stacking sequence and material anisotropy.

Together, these cards allow the shell element to behave like a fully anisotropic laminate with directional stiffness, in-plane shear behavior, and accurate mass distribution. The material coordinate system is defined such that the x-axis aligns with the warp direction and the y-axis with the fill.

3.4.3 Why MAT2 is Used

The `MAT2` card is selected for its ability to represent general orthotropic behavior in shell elements. While alternatives such as `MAT8` exist, they are primarily intended for layered composite definitions and require explicit ply stacking. In this study, the stacking behavior is handled during the homogenization phase using `Jpanel`, so `MAT2` is appropriate for applying the resulting equivalent stiffnesses to a single shell element. [27]

3.4.4 Benefits of the Implicit Shell Model

This modeling strategy provides several key advantages:

- **Efficiency**: It avoids the need for high-resolution meshing of individual tapes or layers, allowing faster simulation runs.

- **Parametric control**: Material properties are directly tied to input parameters such as tape spacing, thickness, and material type.

- **Compatibility with optimization**: The simplified model integrates cleanly with HyperStudy, enabling rapid evaluation of design variants.

- **Sufficient fidelity**: Prior work has shown that this approach captures displacement, mass, and strain trends within engineering accuracy for lattice-based structures.

By using homogenized orthotropic properties in an implicit shell model, the simulation maintains structural insight without incurring the computational cost of geometric resolution. This is essential for the multiscale optimization framework used in this study.

(a) Top-surface alignment

(b) Bottom-surface alignment

Figure 3.8: Shell element offset options in OptiStruct using the ZOFFS parameter in PSHELL. **Left:** The top surface of the shell aligns with the node plane, placing the material centroid below the mesh. **Right:** The bottom surface of the shell aligns with the node plane, placing the centroid above. These offsets are useful when surface-mounted reinforcements (e.g., Weav3D tapes) must be accurately represented in strain response evaluations.

3.5 Homogenization via `Jpanel`

The lattice structure in this study consists of directional thermoplastic prepreg tows placed in warp and fill orientations across the top and bottom surfaces of a composite panel. These tapes create a heterogeneous, asymmetric architecture that is computationally intensive to model discretely. Instead of resolving every tow geometrically, this study uses a homogenization approach implemented through `Jpanel` to generate equivalent orthotropic shell properties.

3.5.1 Purpose of Homogenization

Homogenization is the process of averaging the detailed microstructural behavior of the lattice reinforcement into a set of effective, macroscopic material properties. For composite shells, this means converting the geometric and material definition of each tape (width, thickness, spacing, orientation, number of layers, and material) into an orthotropic stiffness matrix $[Q]$ or MAT2 that captures in-plane and bending behavior across the entire panel region.

This process allows the use of shell elements with directional stiffness without explicitly modeling the individual tows. It significantly reduces model complexity and runtime,

enabling efficient design-of-experiments and optimization workflows.

3.5.2 Jpanel Implementation

`Jpanel` is a command-line homogenization tool that takes in a user-defined input file specifying the panel construction. The core entities defined in the input are:

- `LATTICE` cards: define the tow architecture — including tape spacing, thickness, width, number of layers, and material identifiers for warp (W1/W2) and fill (F1/F2) tows.
- `PPANEL` cards: define panel-level properties such as thickness, number of lattice layers, symmetry flags, bulk material IDs, and shear angles.
- `MAT9OR` cards: define the elastic properties of each constituent material (tapes and bulk) in terms of engineering constants (e.g., E_1, G_{12}, ν_{12}, ρ).

Once these definitions are provided, `Jpanel` computes the through-thickness phase-averaged stiffness and outputs the results in a homogenized material include file.

3.5.3 Output Format and Use

The output of `Jpanel` is a file named `[InputFile]_mat.fem`, which contains:

- `MAT2` cards: orthotropic stiffness matrices for each panel region.
- `PSHELL` cards: property definitions including panel thickness, material linkage, and mass.

These cards replace temporary material definitions in the original model. In HyperMesh, the output file is imported into a base shell model using the `fe-overwrite` import option. This step assigns the homogenized orthotropic properties to the correct shell regions, enabling accurate modeling of bending, membrane, and in-plane shear behavior without resolving each tape.

3.5.4 Why It Matters for This Study

Homogenization via `Jpanel` is the core enabler of this optimization workflow. It allows each design iteration defined by unique tape spacing, layering, and materials to be rapidly converted into a working shell model with engineering-relevant mechanical behavior. Without this tool, exploring such a large design space with discrete modeling would be infeasible.

This homogenized model captures:

- Directional stiffness and anisotropy
- Effects of asymmetry between top and bottom layers
- Influence of tape thickness, width, and spacing on effective panel stiffness and mass

By incorporating both tape and bulk materials into the phase-average laminate formulation, `Jpanel` ensures that even thermally bonded, asymmetric reinforcement architectures can be accurately simulated in OptiStruct with MAT2/PSHELL shell elements.

3.6 Simulation Framework and Model Automation

To enable scalable optimization across a large design space, the simulation workflow must be fully automated. This section explains how simulation inputs are configured, how Jpanel integrates with HyperMesh and OptiStruct, and how templated files are used to manage variable substitution and model assembly.

3.6.1 What Does the Template File Do?

The base simulation input is stored in a template file with a `.tpl` extension. This template acts as a universal version of the OptiStruct input deck, but with embedded parameter tokens (e.g., `#GAP_W#`, `#WTH_F2#`) wherever a variable value is intended to change between runs. These placeholders are automatically replaced with actual values during each design iteration.

The template file ensures that the model setup remains consistent across iterations, while allowing key parameters such as tape spacing, material types, and number of layers to vary systematically.

3.6.2 What Are `.tpl` *and* `.var` *Files?*

- `.tpl` (template) file: contains the structure of the input deck with substitution variables defined as tokens.
- `.var` (variable) file: defines the names and numerical ranges of the parameters to be varied during the optimization or sampling process.

HyperStudy uses the `.tpl` file as a blueprint and fills in each parameter from the current sample point specified in the `.var` file. This results in a customized input file for each design iteration.

3.6.3 What Is Inserted Into the Model?

Once the parameterized input file is written, it is passed to `Jpanel`, which processes the lattice and panel configuration and produces a homogenized include file named `[InputFile]_mat.fem`. This file contains:

- `MAT2` cards: define the orthotropic stiffness and density of the homogenized panel.
- `PSHELL` cards: assign panel thickness and link the shell properties to the finite element mesh.

3.6.4 How Is the Include File Used?

The include file is imported into a pre-built generic model in HyperMesh, typically referred to as the shell panel or start model. This model contains all boundary conditions, loads, and mesh definitions, but uses placeholder material and property definitions. Upon import, the original MAT1/PSHELL entries are overwritten by the homogenized MAT2/PSHELL definitions produced by `Jpanel`, completing the assembly of the simulation-ready model.

3.6.5 Where Does the MAT2 + PSHELL File Go?

In practice, the MAT2 and PSHELL entries from `[InputFile]_mat.fem` are inserted directly into the OptiStruct input deck that is exported from HyperMesh. This input file is then submitted to OptiStruct for solution via the Altair Compute Console or command-line execution.

After solving, OptiStruct generates displacement and strain result files (`.disp`, `.strn`) in ASCII format, which are automatically recognized by the `Jpanel` post-processing routine for further interpretation of panel response including phase-based strains in the reinforcement regions.

3.7 Baseline Panel Configuration

The baseline panel plays a critical role in this study by serving as a reference configuration against which all optimized lattice designs are compared. It enables direct performance benchmarking to evaluate whether lattice-reinforced structures modeled using implicit homogenization and optimized via classical surrogate methods can achieve similar or superior mechanical performance relative to a simpler, continuous composite layout.

This aligns with the core objective of this thesis: to show that conventional surrogate-based optimization workflows, typically used for ply-based composites, remain valid and effective when applied to architected thermoplastic lattices such as those produced by the Weav3D process.

3.7.1 How the Baseline Panel Was Constructed

The baseline model uses the same geometric dimensions, boundary conditions, and loading configuration as the lattice-reinforced panel, ensuring a fair and consistent comparison. However, instead of a spatially varying lattice architecture, the reinforcement is defined as a continuous, quasi-unidirectional shell laminate.

To construct this model, the same `Jpanel` toolchain was used with a modified input. The corresponding `PPANEL` and `LATTICE` definitions were adjusted to represent a fully filled structure with minimized tape spacing and uniform reinforcement across the panel. In this way,

the continuous panel inherits the same MAT2/PSHELL formulation but lacks the spatial anisotropy and material efficiency characteristics of the optimized lattice configurations.

3.7.2 Why This Matters

By evaluating both the optimized lattice configurations and the continuous baseline panel under the same simulation framework, this study can isolate the effects of reinforcement layout. Specifically, it allows us to quantify:

- Whether the optimized lattice can achieve equal or better stiffness and displacement control at lower mass
- The trade-offs between directional stiffness customization and material utilization
- The validity of applying classical optimization strategies to nonuniform, architected structures

Ultimately, the inclusion of the baseline panel validates the practical utility of the optimization framework and highlights the potential for lattice-reinforced composites to reduce weight without compromising structural performance.

3.8 Design of Experiments with Latin Hypercube Sampling

Before optimization can be performed, the design space must be systematically explored to evaluate how performance metrics vary with respect to different combinations of input parameters. This process is carried out using a Design of Experiments (DOE) approach, which samples points across the multidimensional parameter space. [10]

In this study, **Latin Hypercube Sampling (LHS)** [41] was selected as the DOE method. LHS is a statistical sampling strategy that ensures uniform coverage of the design space by dividing each input variable range into equal probability intervals and randomly sampling from each interval exactly once. This leads to a more balanced distribution than purely random sampling, while requiring significantly fewer points than full factorial designs. [49]

3.8.1 Why LHS Was Chosen

LHS is particularly well-suited to surrogate modeling because it:

- Ensures uniform and non-redundant sampling across each variable's range
- Captures both linear and nonlinear interactions between parameters
- Minimizes clustering of sample points in high-dimensional spaces
- Requires fewer simulations to build an accurate model compared to grid-based methods

These characteristics make LHS an efficient and statistically robust method for populating the design space, particularly when simulation cost is high and model evaluations are computationally expensive, as is the case in lattice homogenization and finite element analysis.

In Latin Hypercube Sampling, the range of each design variable x_k is divided into N non-overlapping intervals of equal probability. A single sample is then drawn randomly from each interval, and the samples for all n variables are combined so that each variable is represented exactly once in each interval. [50]

Mathematically, the i-th sample point for variable x_k can be expressed as

$$x_k^{(i)} = F_k^{-1}\left(\frac{p_{ik} - u_{ik}}{N}\right) \tag{3.1}$$

(Adapted from [41]) where F_k^{-1} is the inverse cumulative distribution function of x_k, p_{ik} is a random permutation of the integers $1, 2, \ldots, N$, and u_{ik} is a random number in the interval $(0, 1)$. This ensures that the N samples are uniformly distributed across the range of each variable while avoiding clustering.

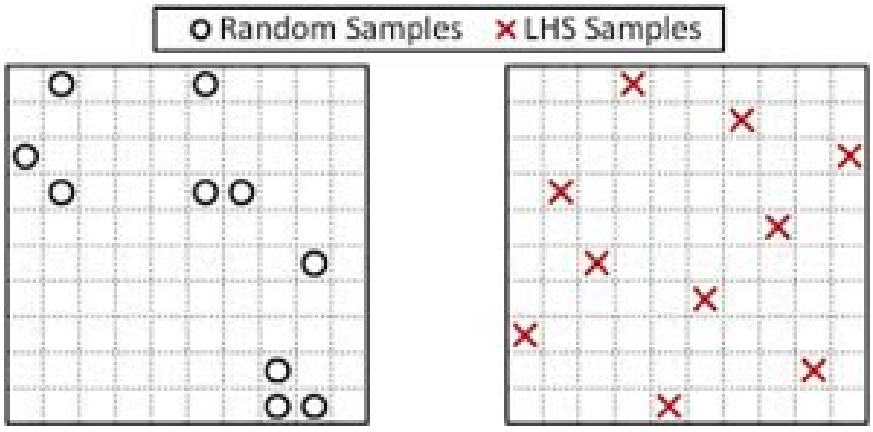

Figure 3.9: Comparison of random sampling (left) and Latin Hypercube Sampling (right) in a two-dimensional parameter space. LHS ensures that each interval along every axis is sampled exactly once, resulting in more uniform and space-filling coverage.[50]

3.9 Surrogate Model Construction with MELS

Once the design space is explored with a lot of iterations using Latin Hypercube Sampling, a surrogate model was developed using these iterations. It connects the input variables and output responses. Instead of running a full element simulation for each design, the surrogate provides a faster way to estimate results

In this framework, the surrogate model is constructed using **Modified Extensible Lattice Sequence (MELS)**, a refined sampling strategy that enhances distribution without duplicating prior samples. This allows the surrogate to better capture local nonlinearities and improve prediction near optimal regions. [25]

3.9.1 Why Surrogate Models Are Used

Direct optimization using high-fidelity simulations is often computationally prohibitive, especially when each model run involves multiscale homogenization and nonlinear structural analysis. Surrogate models offer a way to:

- Evaluate new design configurations in milliseconds

- Enable gradient-free and gradient-based optimization algorithms
- Visualize trade-offs and sensitivity between variables and objectives
- Reduce total simulation time while preserving predictive accuracy

3.9.2 Why MELS Was Chosen

The MELS method is preferred in this study because it:

- Accurately captures trends in structural responses
- Supports extrapolation near the boundaries of the design space
- Integrates seamlessly with HyperStudy's optimization engine
- Provides good fit metrics (e.g., R^2 values) for model validation

Once the surrogate is trained, its fidelity is verified through internal metrics such as the coefficient of determination and root mean squared error. The coefficient of determination is defined as

$$R^2 = 1 - \frac{\sum_{i=1}^{n}(y_i - \hat{y}_i)^2}{\sum_{i=1}^{n}(y_i - \bar{y})^2} \tag{3.2}$$

(adapted from [15]) where y_i are the simulation results, $\hat{y}_i$ are the surrogate predictions, and $\bar{y}$ is the mean of the simulation results. The root mean squared error is given by

$$\text{RMSE} = \sqrt{\frac{1}{n}\sum_{i=1}^{n}(y_i - \hat{y}_i)^2} \tag{3.3}$$

A high R^2 (close to 1) and a low RMSE indicate that the surrogate captures the variance in the simulation data with minimal error. [45]

3.10 Optimization Using the Global Response Surface Method (GRSM)

After constructing the surrogate model, the next step is to identify the optimal design point which is the combination of lattice parameters that minimizes mass while satisfying strain constraints. This is achieved using the **Global Response Surface Method (GRSM)**.

3.10.1 What GRSM Does

GRSM explores the design space by sampling and evaluating points on the surrogate response surface, rather than using the full finite element solver for every iteration. It uses a blend of global exploration and local refinement to identify the best candidate solutions based on the predicted response values. [6]

Key characteristics of GRSM include:

- Sampling from the full parameter space, not just around local optima
- Adaptive refinement based on surrogate trends and fit quality
- Ability to operate without requiring gradients or derivative information
- Support for both continuous and discrete variables

3.10.2 Why GRSM Was Selected

GRSM is particularly well-suited for surrogate-based workflows involving complex, nonlinear, or multi-modal response surfaces such as those arising in homogenized composite lattice structures [57]. It was selected in this study because:

- It performs well with surrogate models constructed from **Latin Hypercube Sampling (LHS)** and refined using **MELS**, ensuring that surrogate accuracy is leveraged during optimization.
- It avoids premature convergence to local minima by sampling across the entire design domain.
- It is computationally efficient, evaluating only the surrogate model rather than re-running expensive simulations.

- It integrates directly with the HyperStudy environment and its adaptive sampling strategy.

3.10.3 Visualization of GRSM Operation

Figure 3.10 conceptually illustrates how GRSM operates on a response surface generated from Latin Hypercube and MELS samples. The algorithm samples across the full domain, refines near-optimal regions, and iteratively converges on the best solution.

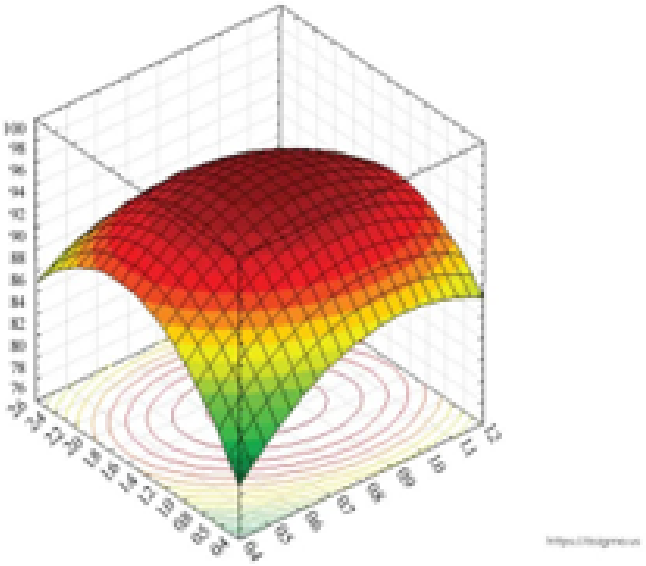

Figure 3.10: Conceptual diagram of GRSM operating on a surrogate response surface. Points are sampled across the full design space (from LHS and MELS), and the optimal solution is identified without re-solving the high-fidelity model. Adapted from [56].

The optimization problem solved by GRSM can be expressed as

$$\min_{\mathbf{x}\in\mathcal{D}} f(\mathbf{x}) \quad \text{s.t.} \quad g_j(\mathbf{x}) \leq 0,\ j = 1, \ldots, m \tag{3.4}$$

(Adapted from [55]) where $\mathbf{x}$ is the vector of design variables (warp and fill spacings), $f(\mathbf{x})$ is the objective function (panel mass), and $g_j(\mathbf{x})$ are the constraint functions (e.g., maximum

tensile strain limit).

Instead of evaluating $f(\mathbf{x})$ directly from the high-fidelity finite element solver, GRSM operates on the surrogate approximation $\hat{f}(\mathbf{x})$ constructed from the DOE data,

$$\hat{f}(\mathbf{x}) \approx f(\mathbf{x}) \tag{3.5}$$

allowing the search process to explore the design space efficiently and refine near-optimal regions without incurring the full simulation cost at each iteration.

Chapter 4

HYPERSTUDY EXECUTION AND OPTIMIZATION IMPLEMENTATION

This chapter details the execution framework developed in Altair HyperStudy to optimize a lattice-reinforced composite panel using experimentally measured material properties. Building on the parameter definitions and surrogate modeling methodology introduced in earlier chapters, the workflow transitions from conceptual design to full implementation, showing how design variables are linked to simulation models, how solver input files are generated, and how objectives and constraints are applied across automated design iterations.

The optimization problem seeks to minimize the structural mass of the panel while limiting the maximum tensile strain to 3430 $\mu\varepsilon$ in a three-point bending load case. Material properties for all finite element models are derived from digital image correlation (DIC) testing of coupon specimens, ensuring that simulations capture realistic behavior rather than relying on nominal datasheet values. A surrogate-based workflow is used to evaluate a wide range of lattice configurations efficiently, exploring how parameters such as tow spacing, material selection, and number of layers influence overall performance.

While theoretical expectations suggest that warp-aligned reinforcement should dominate due to the direction of the applied bending load, this framework does not assume that outcome. Instead, it formally evaluates and quantifies the influence of lattice reinforcement strategies, including those enabled by the Weav3D process, on stiffness-to-weight performance relative to conventional laminates. The sections that follow describe how the HyperStudy environment integrates parameterization, homogenization, solver automation, and post-processing to achieve these goals.

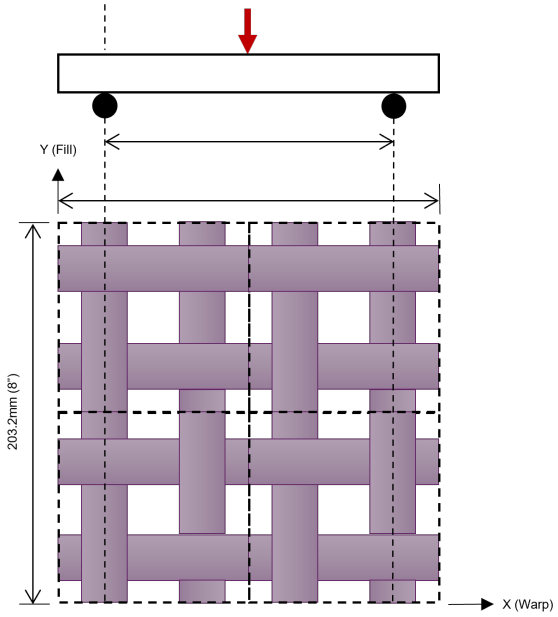

Figure 4.1: Bending Load Case

4.1 Overview of HyperStudy Execution

Altair HyperStudy serves as the central driver for design exploration, parameter variation, and optimization in this study. Its primary role is to manage the flow of information between the design variables, the surrogate modeling layer, and the simulation solvers, enabling fully automated evaluation of dozens of lattice configurations without manual intervention.

The execution framework begins with a parameterized input file defined through a `.tpl` template. HyperStudy substitutes user-defined design variables into this file to create a unique finite element model input for each design point. These input files are then processed by `Jpanel`, which homogenizes the material (from DIC testing) and lattice definitions and produces equivalent material properties in the form of `MAT2` and `PSHELL` cards. These are inserted into a base shell model in HyperMesh, which is exported as a complete OptiStruct input deck and submitted for solution.

Upon completion of each simulation, the displacement and strain results are automatically post-processed using `Jpanel`'s post module. This produces a formatted results file from which HyperStudy extracts target metrics such as mass and tensile strain. These values are

used to evaluate the objective function and enforce constraints for each design iteration.

This modular, dual-step approach: Jpanel for material homogenization and OptiStruct for structural simulation allows for systematic design space exploration while maintaining engineering fidelity.

HyperStudy Automation Workflow

1. Import Template

- `.fem` file converted to `.tpl` for parameter insertion
- Parameterized design variables defined using tokens (e.g., #GAP_W#)

2. Invoke `Jpanel`

- Custom solver script runs `jpanel.exe pre`
- Outputs homogenized material file: `_mat.fem`

3. Insert Material Include

- Conditional logic inserts `_mat.fem` into shell model
- Overwrites PSHELL/MAT1 with homogenized MAT2 properties

4. Run Simulation

- Launch OptiStruct via HyperStudy
- Evaluate displacement, strain, and mass response

5. Collect Responses

- HyperStudy extracts output from post-processed files
- Ready for DOE, Sampling Fit, and Optimization

4.2 Input Structure and Parameter Substitution

The simulation workflow is driven by a template-based input system, where a parameterized OptiStruct file (`.tpl`) is used to define the model configuration. This template is derived

from a standard OptiStruct input deck and includes placeholder tokens representing design variables such as tow widths, gap spacings, and material selections.

HyperStudy manages these variables through an associated `.var` file, which assigns real numeric values to each parameter during every design iteration. At runtime, the tool substitutes these values into the template to generate a complete OptiStruct input file (`Input_Main.fem`) tailored to the current design point.

This file is then passed into the Jpanel homogenization module, enabling automated generation of homogenized material models without manual editing. The approach allows for fast and repeatable evaluation of different lattice configurations using a consistent input structure across all simulation runs.

4.3 JPanel Card Structure and Baseline Configuration

4.3.1 MAT9OR – Orthotropic Material Definition*

To model the orthotropic behavior of the lattice constituents, the input template defines each phase using a `MAT9OR*` card. This format captures direction-dependent mechanical properties and is used by Jpanel to construct homogenized material models for the composite. These cards are populated from our material testing using DIC.

While the homogenization process can also output the orthotropic stiffness matrix in MAT9OR format, the data is converted to MAT2 for use in the finite element model. This is because OptiStruct's PSHELL property definitions require separate membrane and bending stiffness terms, which are directly supported by MAT2. The conversion ensures compatibility with shell modeling and allows the homogenized laminate behavior to be represented accurately in the structural analysis.

Material ID 2 – Carbon:

```
MAT9OR*               2 9.450000000E+04 4.200000000E+03 4.200000000E+03  Carbon
*        3.500000000E-01 0.156000000E-01 0.156000000E-01 1.310000000E-03
*        1.300000000E+03 2.840000000E+03 1.300000000E+03-6.000000000E-07
*        4.000000000E-05 0.000000000E+00
```

Each line encodes key orthotropic material properties:

- **Line 1:** Material ID, elastic moduli (E1, E2, E3), and name
- **Line 2:** Poisson's ratios (ν_{12}, ν_{23}, ν_{31}), and Mass density
- **Line 3:** Shear moduli (G12, G23, G31) and thermal expansion coefficient in the 1-direction (fiber direction)
- **Line 4:** coefficient of thermal expansion in the 2 and 3 direction (matrix transverse direction and through-thickness direction)

4.3.2 LATTICE – Tape Architecture Definition*

The `LATTICE*` card defines the reinforcement layout, including material IDs, tape widths and thicknesses, number of tows, and gap spacings. This allows Jpanel to build a homogenized representation of the woven structure.

Baseline LATTICE* definition:

```
LATTICE*              1        Lattice1 0.000000000E+00 0.000000000E+00
*                     2 5.000000000E-01               1 1.000000000E+00
*                     2 5.000000000E-01               1 1.000000000E+00
*                     2 5.000000000E-01               1 1.000000000E+00
*                     2 5.000000000E-01               1 1.000000000E+00
*                     5
```

This configuration represents:

- All warp and fill tapes used only Carbon (Material ID 2)
- `GAP_W` and `GAP_F` were set to 0.0 to simulate a continuous composite
- Tape widths set to 1.0 mm, thicknesses to 0.5 mm (0.25 x 2 tapes) for all tows
- Number of tows per direction set to 1 for simplicity
- Bulk matrix material assigned as Polypropylene (PP), included only to meet card definition requirements but not structurally relevant

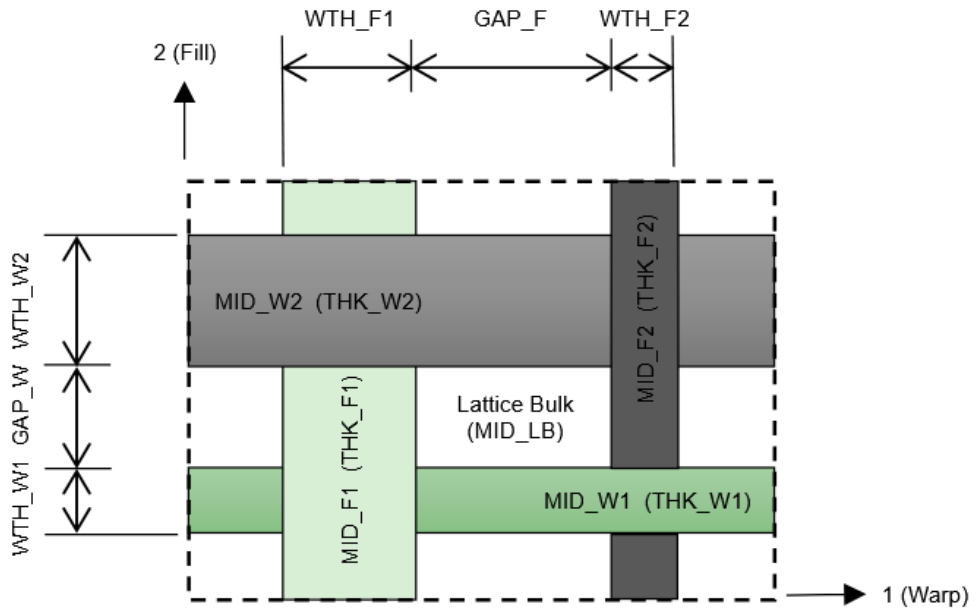

Figure 4.2: Schematic representation of Weav3D lattice configuration, showing warp and fill tow placements, tape widths (`WTH`), gaps (`GAP`), and corresponding material IDs (`MID`) and thicknesses (`THK`). The bulk region is denoted as `MID_LB`.

4.3.3 PPANEL – Panel Stackup Definition*

The `PPANEL*` card defines how the lattice is assembled into a full panel. It specifies symmetry, total thickness, number of layers, and bulk regions.

Baseline PPANEL* definition:

```
PPANEL*                 1          Panel1         Weav3D
*                       2            true           true
*        5.000000000E+00-2.500000000E+00              0               0
*                       5 5.000000000E-01
```

Key parameters used:

- **LID = 2**, **NUM_L = 1**: one lattice layer
- **SYM = true**: symmetric about the mid-plane
- **BOT = true**: lattice appears on both top and bottom surfaces

- **THK = 5.0 mm**, **Z0 = -2.5 mm**: panel centered around neutral axis
- **PHI = 0**, **NSM = 0**: no shear angle or added mass
- **MID_BC = MID_BS = 5**: PP bulk for both core and skin
- **VOL_BS = 0.5**: equal thickness bulk skin layers

This structure produces a clean, symmetric panel compatible with the homogenized workflow and serves as the reference for optimization.

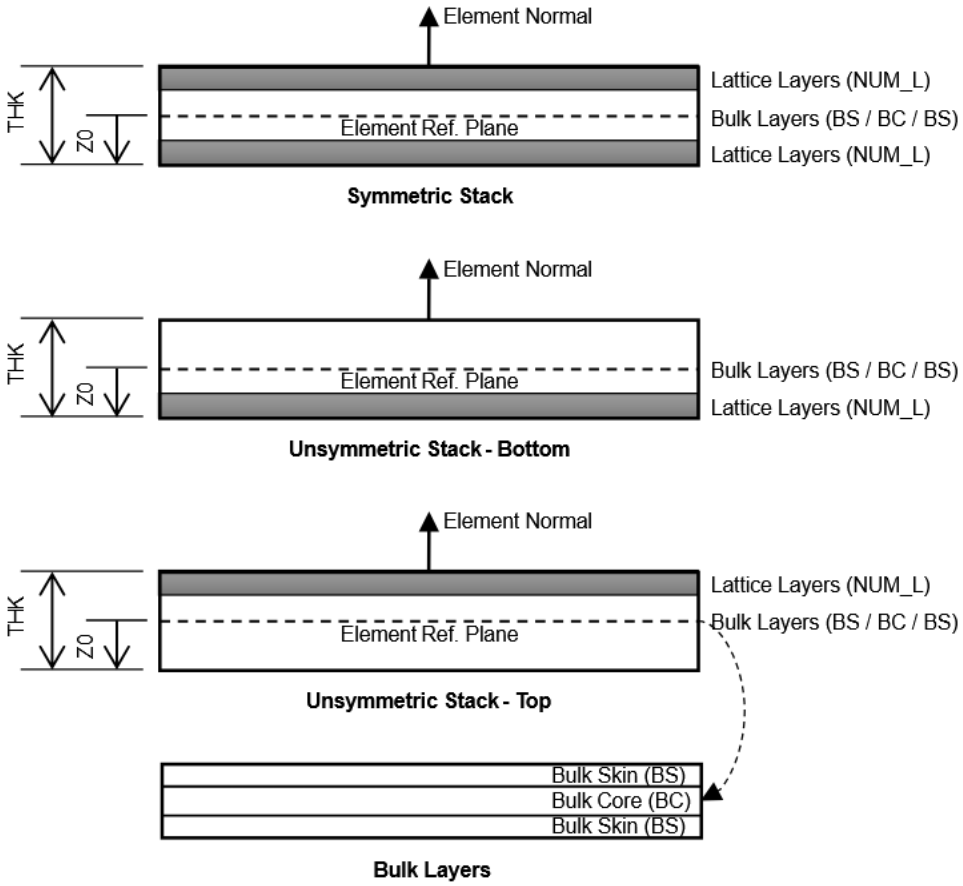

Figure 4.3: PPANEL stacking configurations. The symmetric stack places an equal number of lattice layers (`NUM_L`) above and below the bulk layers. The unsymmetric configurations allow lattice reinforcement to be concentrated either below or above the bulk layers. The bulk layers consist of a sandwich structure: Bulk Skin (BS), Bulk Core (BC), and Bulk Skin (BS). The position of the element reference plane is governed by the value of `Z0`.

4.3.4 Baseline Panel Setup

The baseline configuration was modeled as a flat rectangular shell panel with the following dimensions:

- Length: 127 mm (span direction)
- Width: 177.8 mm (load distribution direction)
- Thickness: 5.0 mm (defined via `PPANEL*`)

The panel was meshed using structured CQUAD4 shell elements to ensure sufficient resolution of bending behavior. Boundary conditions replicate a three-point bending test:

- **Supports:** Simply supported along both shorter edges using single-point constraints (SPCs) to restrict Z-direction motion while allowing in-plane freedom.
- **Loading:** A distributed vertical load is applied at midspan using 21 multi-point constraints (MPCs), which couple a reference loading node to a line of underlying nodes. This approximates a roller-type head and ensures uniform force distribution.

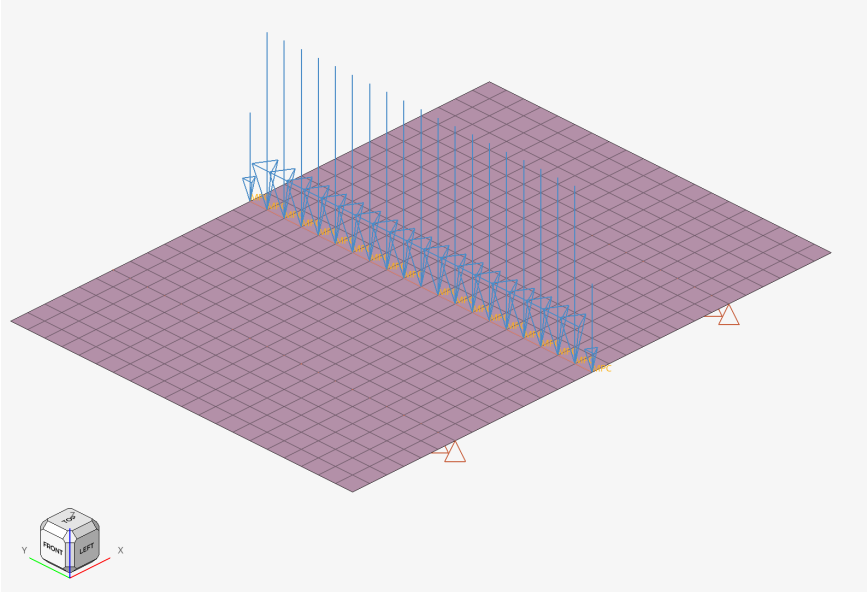

Figure 4.4: Finite element model of the baseline panel. The panel is simply supported at both shorter ends and loaded at midspan via a distributed vertical force applied using 21 MPC elements. The mesh consists of structured CQUAD4 shell elements.

4.3.5 Homogenized Material Output

After substituting the selected parameters into the input template, the `jpanel.exe pre` process converts the lattice and panel definitions (MAT9OR) into a set of homogenized material and property cards compatible with OptiStruct. For each panel configuration, Jpanel generates one `PSHELL` card and four corresponding `MAT2` cards. These represent the directional stiffness components of the structure: membrane, bending, transverse, and coupling behavior.

The `MAT2` entries capture anisotropic elastic properties derived from the multiscale homogenization process, allowing the model to represent the directional response of the composite without explicitly modeling individual tows or layers. Each `PSHELL` card links a specific panel thickness to the appropriate homogenized stiffness matrices defined in the `MAT2` entries.

```
PSHELL*      1      100000001     4.000000000E+00           200000001
*            1.000000000E+00           300000001     1.000000000E+00     0.000000000E+00
*            0.000000000E+00     1.000000000E+00           400000001
MAT2*              100000001     1.945370321E+04     1.086543662E+03     0.000000000E+00
*            1.125472306E+04     0.000000000E+00     1.113165963E+03     1.100529714E-03
*            7.343326213E-06     1.526577662E-05     0.000000000E+00
```

In this example, `MAT2` ID 100000001 defines membrane stiffness, while IDs 200000001 through 400000001 represent bending, transverse, and coupling responses, respectively. These values are generated internally by Jpanel using the provided geometry and material inputs. During each HyperStudy iteration, the corresponding homogenized properties are updated automatically, ensuring consistency between the design parameters and the structural model throughout the optimization process.

4.4 Solver Execution and Post-Processing

Once Jpanel generates the homogenized material model, it is inserted into a generic finite element model via INCLUDE referencing. The updated deck is then submitted to OptiStruct for linear static analysis representing a three-point bending test with simple supports and a central concentrated load.

The solver input deck uses a standard setup:

```
$HMNAME LOADSTEP* "BendWarp"
LABEL BendWarp
ANALYSIS STATICS
SPC = 6
LOAD = 7
MPC = 8

OUTPUT,H3D,FL
OUTPUT,OPTI,FL
DISPLACEMENT = ALL
ELFORCE = ALL
STRAIN = ALL
STRESS = ALL
```

OptiStruct produces a variety of result files for each run:

- `.h3d` — field data (displacement, stress, strain)
- `.stat` — total mass and property-level breakdown
- `.out` — solver convergence, warnings, runtime info

These entries ensure that all relevant data, nodal displacements, element forces, and strain fields are written to the `.h3d` results file. The total panel mass is obtained from the `.stat` file, which reports weight and volume by property ID.

Post-processing is handled through `jpanel.exe post`, which parses the OptiStruct outputs (`.disp`, `.strn`) and generates a homogenized ASCII file (`.hwascii`). Strain is extracted at the panel midspan to reflect maximum deformation under bending. This output is returned to HyperStudy, where strain is evaluated as a constraint and mass is treated as the objective function.

Although individual tows are not resolved in the finite element mesh, the homogenized behavior defined by `Jpanel` captures directional stiffness effects from warp and fill reinforcement. The strain and stress outputs represent the averaged response of the full structure,

allowing performance comparisons across design iterations.

Because the material definitions retain phase-specific orientation and stacking logic, the homogenized fields can be interpreted in the context of the original lattice architecture. For example, in several optimal cases, fill tows were removed entirely without exceeding strain limits indicating that under bending-dominant loading, fill reinforcement may be structurally redundant.

This reinforces the effectiveness of homogenized multiscale modeling in guiding design simplification, without the computational burden of explicit tow-level resolution.

4.5 Constraints, Objectives, and Optimization Setup

The optimization problem is defined with mass minimization as the objective and strain limited to 3430 microstrain as the constraint. These targets were selected to balance lightweight design with allowable deformation under load and to showcase if conventional optimization strategies work with Weav3D's methodology.

The design variables being used will be warp and fill spacings. Tape width and thickness are held constant based on manufacturing constraints. Each tow is assumed to be 1.0 mm wide and 0.25 mm thick, stacked in two layers per face to produce a 0.5 mm contribution per side. These values were not included in the optimization space.

Warp and fill spacing were varied between 0 mm and 100 mm, where 0 mm represents a fully continuous panel and 100 mm represents a configuration with minimal reinforcement. These limits were selected to explore the entire practical design space while remaining manufacturable.

HyperStudy evaluates each design using the automated simulation chain. Mass values are parsed from the `.stat` file, and midspan strain is extracted from the `.hwascii` results. If the strain exceeds 3430 microstrain, the design is rejected. Otherwise, the optimizer proceeds based on gradient-free methods to reduce the structural mass while satisfying performance constraints.

Chapter 5

RESULTS & EXECUTION

This chapter presents the structural performance outcomes obtained from the lattice optimization study. Using the automated HyperStudy–Jpanel–OptiStruct workflow described in Chapter 4, various design configurations were evaluated with mass minimization as the objective and a maximum allowable strain constraint of 3430 $\mu\varepsilon$

The results highlight how warp and fill spacing, material selection, and the number of lattice layers affect mechanical efficiency under three-point bending. In particular, the study evaluates whether lattice-based reinforcement using Weav3D technology can match or outperform a baseline continuous panel while offering weight reductions. Observed strain distributions, mass trends, and parameter sensitivities are discussed, along with how they align with theoretical expectations.

The baseline configuration is first used to establish reference strain and mass values. Following this, optimized lattice panels are compared to identify structural trade-offs and to assess the redundancy or necessity of certain reinforcement directions under bending-dominant loading.

5.1 Overview of Simulation Results

Each design point generated in the optimization workflow was post-processed to extract two key metrics: total structural mass and midspan tensile strain. These results were filtered to ensure compliance with the strain constraint and were then analyzed to identify trends and dominant design features.

A continuous panel constructed from quasi-unidirectional plies served as the baseline reference. This baseline was simulated under the same boundary and loading conditions, enabling direct performance comparison with lattice-reinforced configurations. The optimized lattice structures are evaluated against this benchmark to quantify weight savings

and to determine whether directionally tailored reinforcement offers performance benefits under bending.

The following sections present detailed plots of strain and mass distributions across the design space, as well as optimization paths, parameter sensitivities, and selected design outcomes.

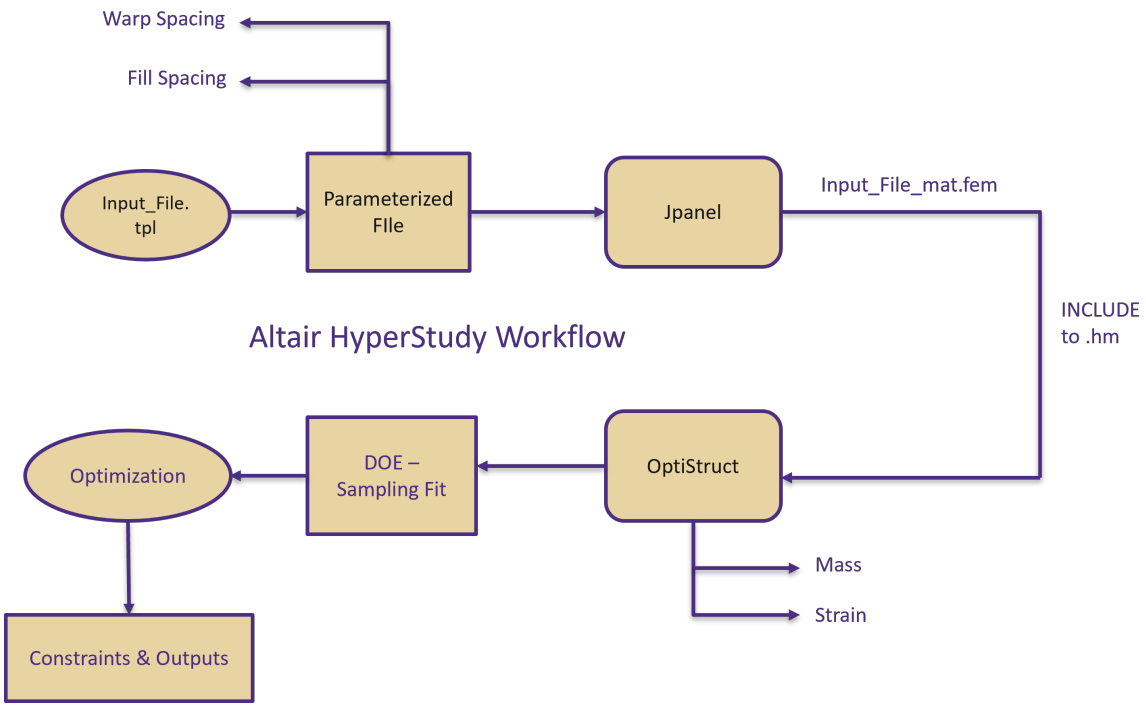

Figure 5.1: Detailed HyperStudy optimization workflow flow chart

5.2 Baseline Panel Simulation Results

The baseline panel, defined using homogenized carbon-only reinforcement with zero warp/fill gaps and minimal tape widths, was evaluated under three-point bending using the simulation setup described in Chapter 4.

A nominal vertical load of 111.21 N was applied at midspan using 21 MPC-linked nodes. Reaction forces at both supports confirmed equilibrium, with each end supporting approximately 111.21 N.

The resulting peak strain at midspan was recorded as [3430 $\mu\varepsilon$] and the corresponding

structural mass was [138 g], forming the reference case for all comparative optimization evaluations.

This configuration serves as a control panel, allowing for direct benchmarking of mass and strain against all lattice-optimized designs in the following sections.

5.2.1 Contour Visualizations

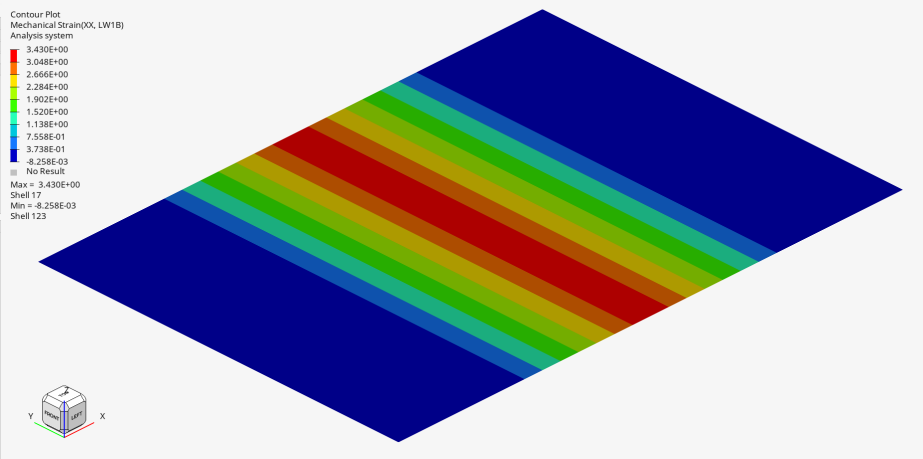

Figure 5.2: Strain in XX direction (LW1B)

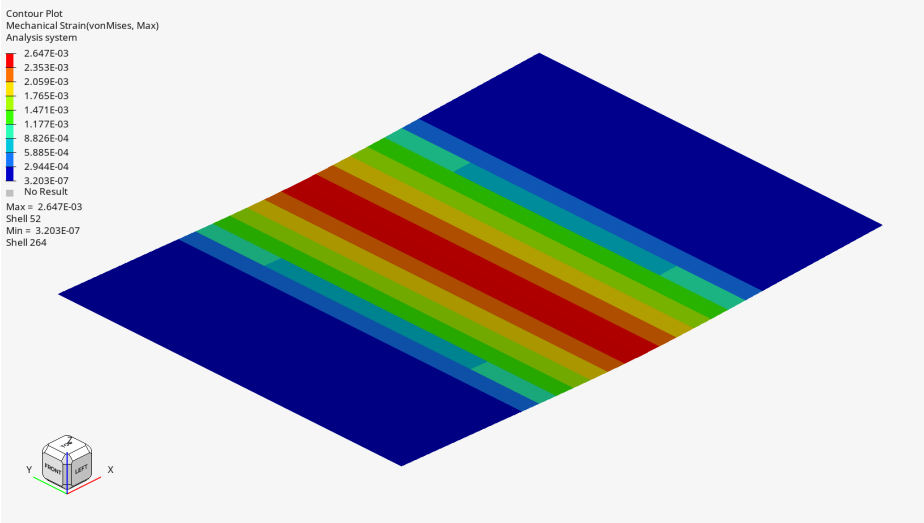

Figure 5.3: von Mises strain distribution under central load

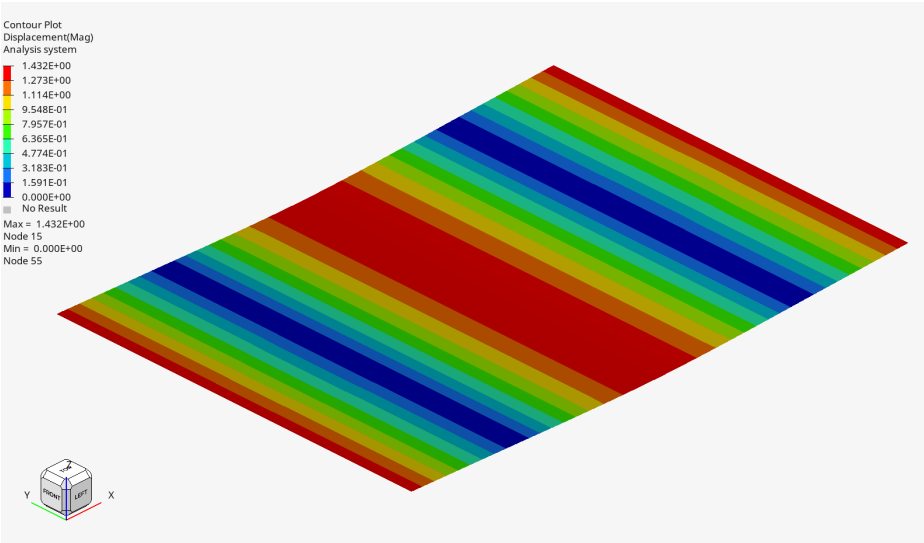

Figure 5.4: Total displacement magnitude across the panel

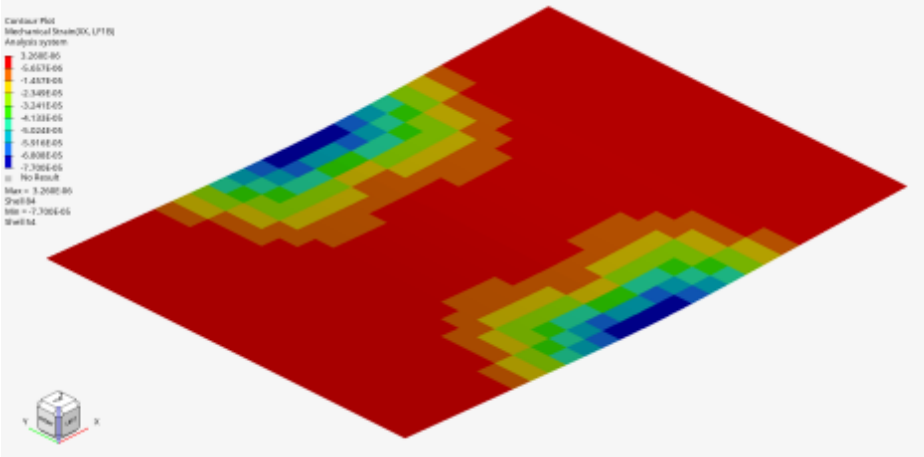

Figure 5.5: Strain in YY direction (LF1B)

Among the available strain outputs, the `LW1B` field in the XX direction was selected as the constraint for optimization. This direction corresponds to the outermost fiber strain in the warp direction, which is critical in a three-point bending configuration like the one modeled here. Since bending induces maximum tensile and compressive strains at the top and bottom surfaces along the panel length, `LW1B` provides a meaningful measure of structural performance. The maximum observed strain was approximately 3.43×10^{-3}, or 3430 microstrain.

Table 5.1 summarizes the key outputs for the baseline panel. Results include von Mises strain, directional strain (XX), and displacement magnitude.

Table 5.1: Summary of simulation results for the baseline panel

Result Type	**Max Value**	**Min Value**	**Max Location**	**Min Location**
Max von Mises Strain	2.647×10^{-3}	3.203×10^{-7}	Shell 52	Shell 264
Max Displacement (Magnitude)	1.432 mm	0.000 mm	Node 15	Node 55
Max Strain XX (LF1B)	3.260×10^{-6}	-7.700×10^{-5}	Shell 84	Shell 54
Max Strain XX (LW1B)	3.430×10^{-3}	-8.258×10^{-6}	Shell 17	Shell 123

5.3 Design of Experiments (DOE)

To efficiently explore the influence of input parameters on structural performance, a Design of Experiments (DOE) study was conducted using Latin Hypercube Sampling (LHS). This method ensured uniform coverage of the design space with a manageable number of simulations.

The DOE focused on understanding how warp and fill spacing, tape width, and thickness affect structural mass and midspan strain under bending. These results served as input for HyperStudy's surrogate model (Sampling Fit), allowing for rapid approximation of response trends without rerunning full simulations.

The DOE phase also revealed parameter sensitivities. Variables such as fill spacing and fill-layer counts showed minimal impact and were excluded from subsequent optimization, reducing dimensionality and improving convergence efficiency.

Key DOE results are summarized below, forming the foundation for the surrogate modeling and global optimization process.

Table 5.2: Five random DOE Trials

Parameter	**Trial 19**	**Trial 62**	**Trial 8**	**Trial 73**	**Trial 43**
WARP_SPAC	10.82	75.84	84.16	19.99	29.05
FILL_SPAC	20.96	20.29	86.1	4.84	11.48
Mass (g)	135.11	103.34	88	148.53	146.59
Strain ($\mu\varepsilon$)	3637	9331	7339	2581.33	2708.49

These representative DOE results form the basis for the next phase, which involves sampling fit and surrogate modeling. This ensures that the response trends across the design space are well captured. These points are used to train a response surface model in HyperStudy.

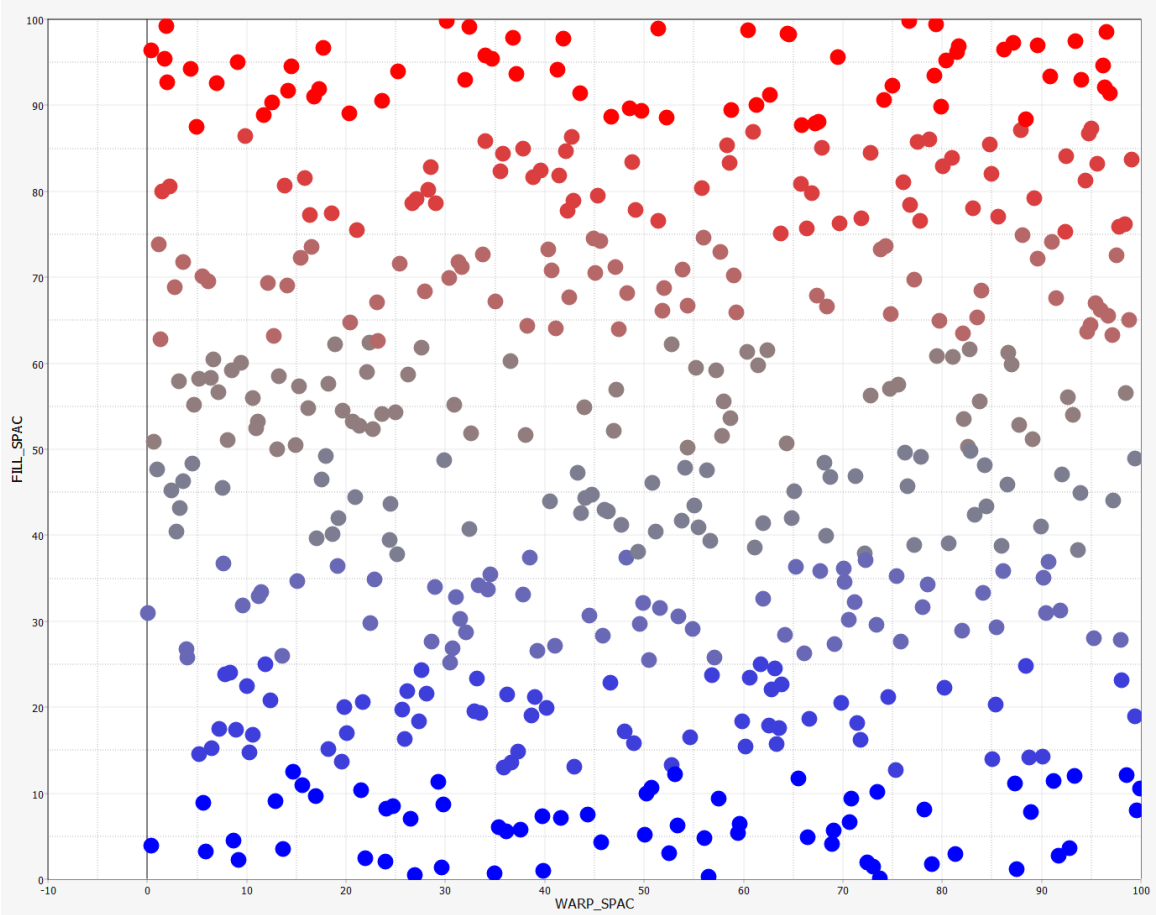

Figure 5.6: Design of experiments scatter plot illustrating the distribution of sampled points for warp spacing and fill spacing. Bubble colors indicate the dominant reinforcement orientation, with red for fill-dominated and blue for warp-dominated cases.

5.4 Sampling Fit

The Design of Experiments provided valuable insights into how the key parameters influence structural responses. However, performing finite element analyses for every possible combination of design parameters is computationally impractical. To address this, we apply a Sampling Fit approach using the DOE results to develop a surrogate model in HyperStudy. This surrogate approximates structural responses such as mass and strain across the design space with high accuracy, enabling rapid evaluations without rerunning simulations.

In addition to supporting optimization, the surrogate model allows us to perform detailed sensitivity analysis, revealing which parameters have the greatest influence on performance. This insight helps streamline the design space by identifying and removing variables that have minimal or no impact, improving computational efficiency while maintaining fidelity. By reducing dimensionality and guiding design decisions, the surrogate model becomes a critical tool in both optimization and interpretation.

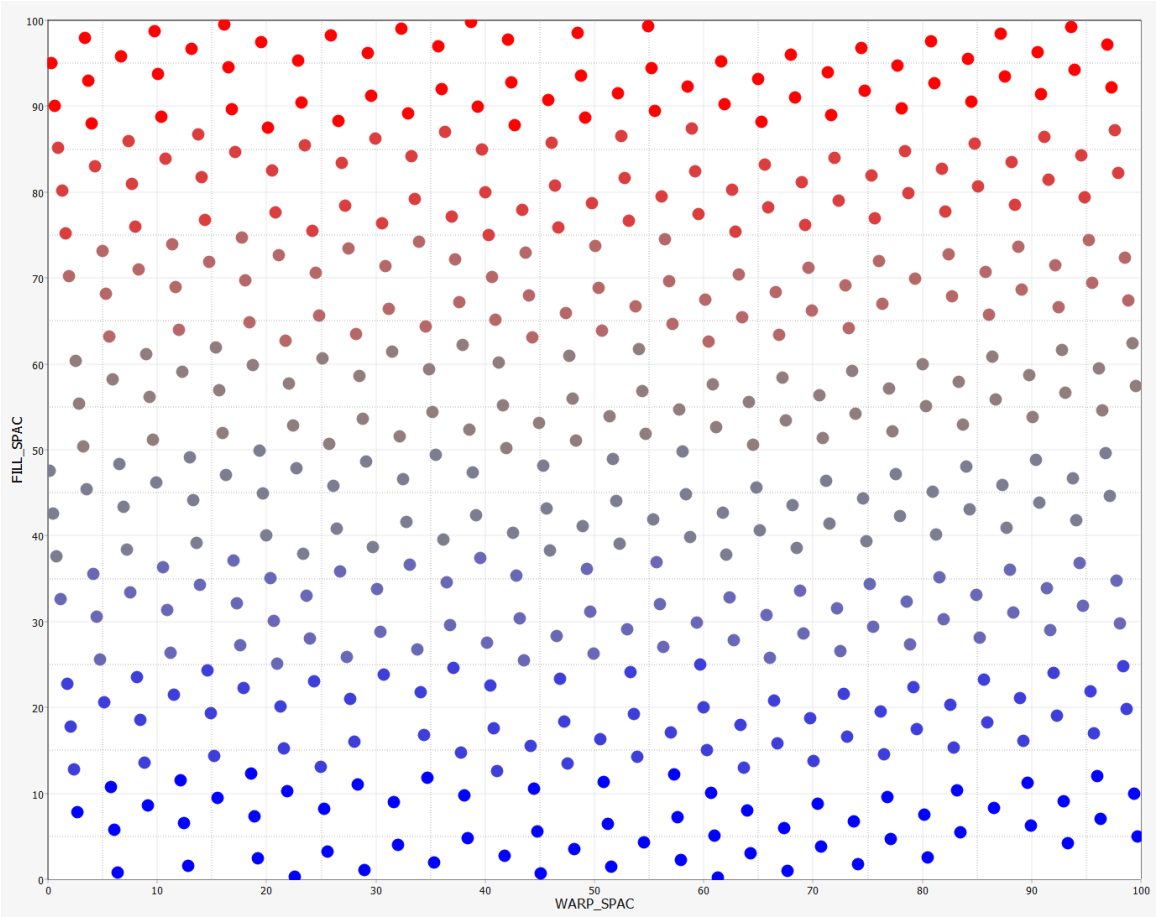

Figure 5.7: Surrogate model fit for warp and fill spacing, showing the same design space with predicted trends overlaid. Bubble colors again indicate the dominant reinforcement orientation, distinguishing fill-dominated (red) from warp-dominated (blue) configurations.

The resulting surrogate response surface for maximum tensile strain, along with the

corresponding sampling points, is shown in Figure 5.8.

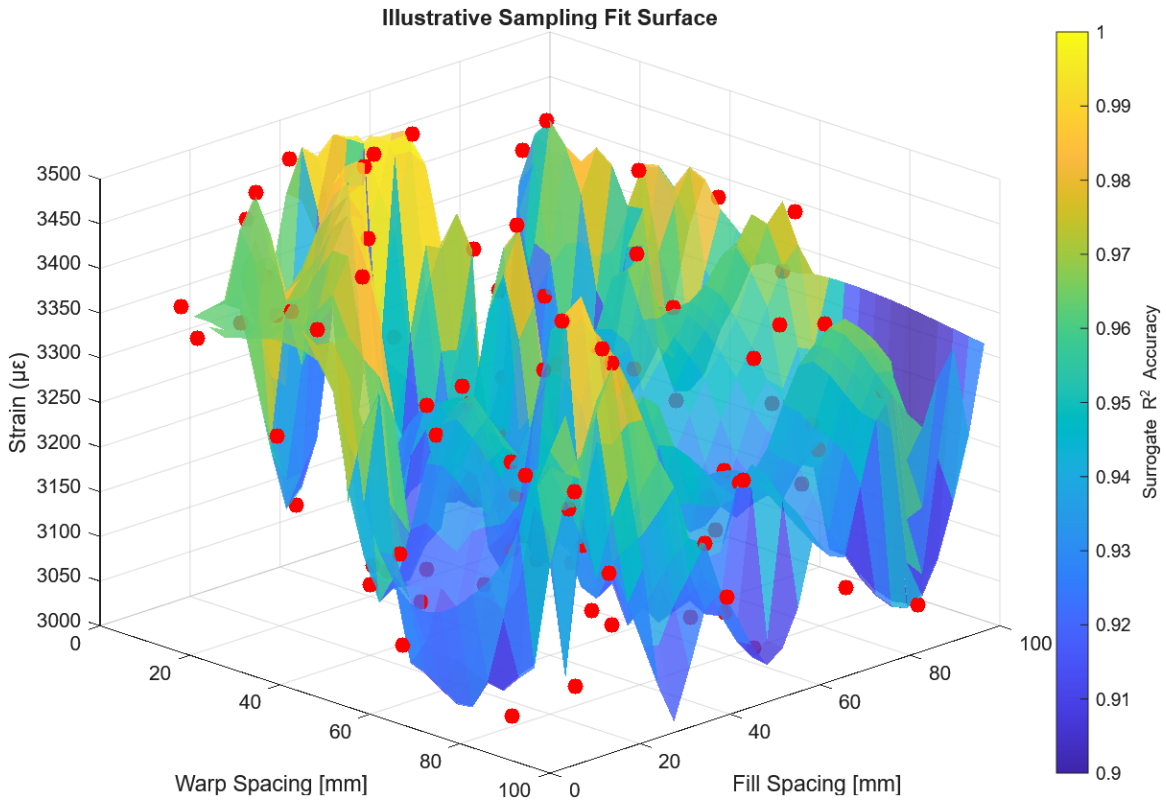

Figure 5.8: Sampling Fit surface for maximum tensile strain as a function of warp and fill spacing. The surface represents the surrogate model predictions, while the red points indicate the DOE sampling locations used for model training. Color scale denotes local surrogate R^2 accuracy, with warmer colors indicating higher agreement between surrogate predictions and high-fidelity simulation results.

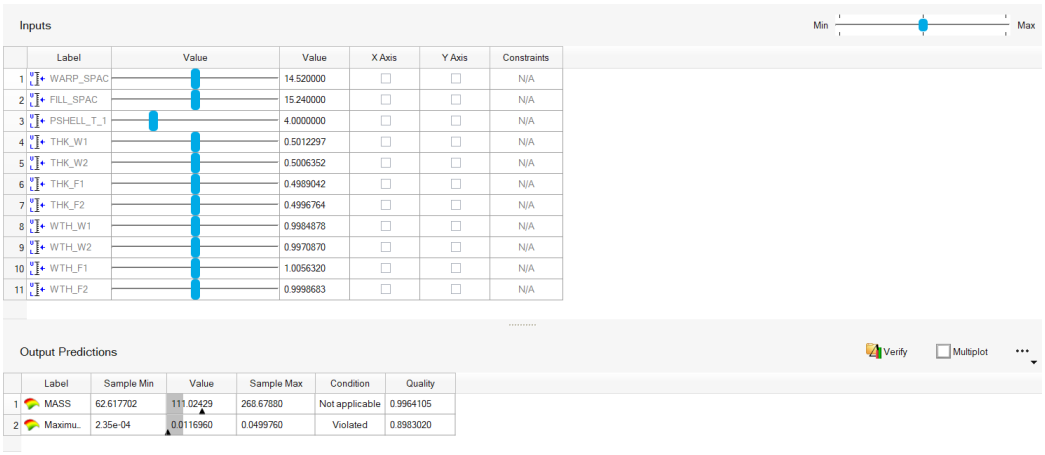

Figure 5.9: Trade-off visualisation produced from the Sampling Fit surrogate model. This plot highlights the balanced region of the design space in which the target strain is satisfied while mass is minimised, providing immediate guidance for the subsequent optimisation task.

5.5 Optimization Results

The purpose of this optimization study is not merely to minimize mass or satisfy a performance constraint, but to evaluate whether classical surrogate-based optimization strategies can adaptively simplify an architected structure such as a lattice-reinforced composite panel. The goal is to observe whether HyperStudy naturally removes unnecessary reinforcement and converges toward a structurally efficient, lightweight configuration while maintaining acceptable strain levels.

With the surrogate model trained on Latin Hypercube data and the design space reduced to its most influential parameters, the optimization phase was executed using Altair HyperStudy's global response surface methodology. Warp and fill spacing were treated as variable inputs, while tape dimensions remained fixed due to manufacturing constraints. By tracking the algorithm's convergence behavior, we assess whether traditional optimization logic can be applied effectively to lattice-based composites modeled through homogenized material definitions.

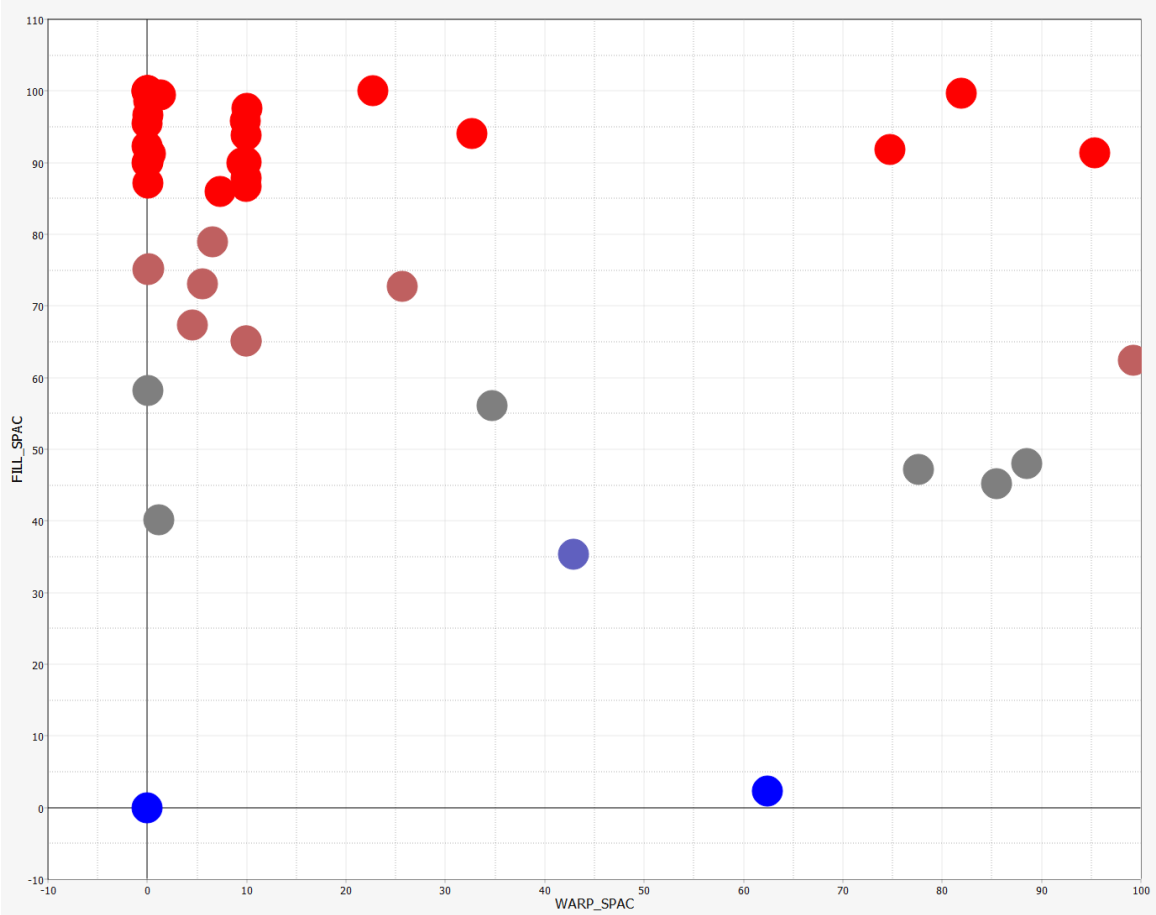

Figure 5.10: Two-dimensional scatter plot showing the relationship between warp spacing and fill spacing

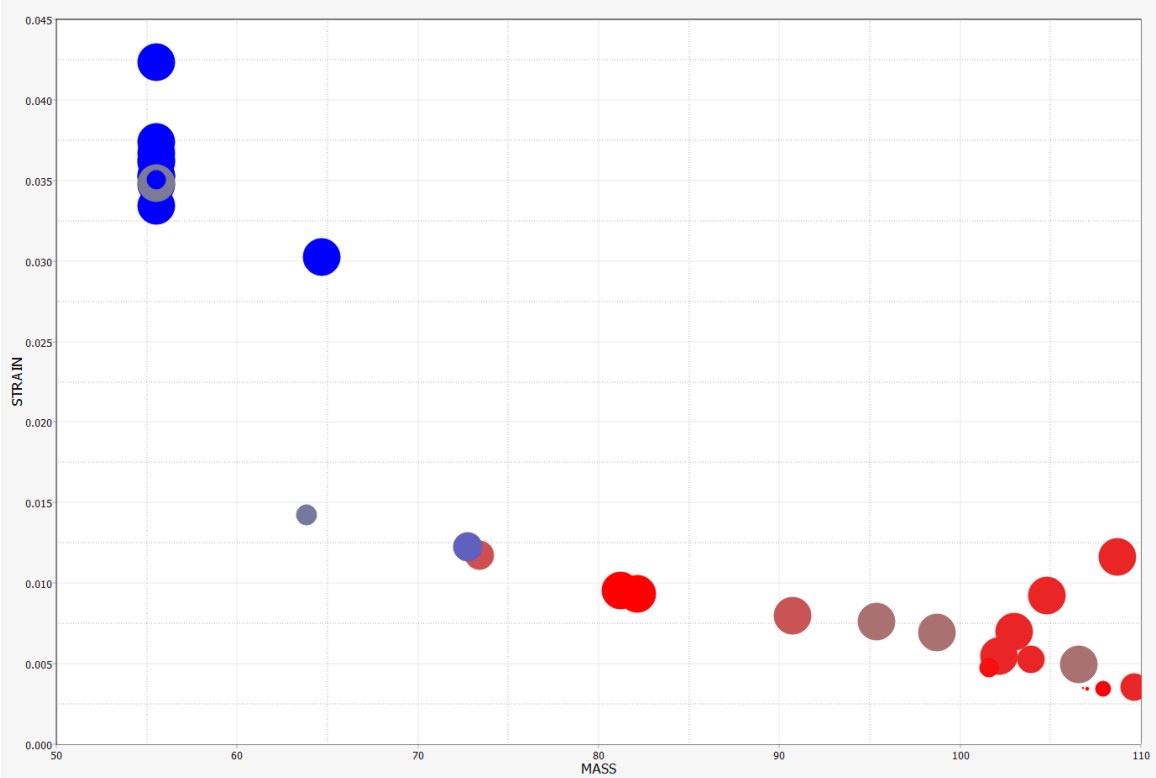

Figure 5.11: Two-dimensional scatter plot showing the relationship between mass and strain

From the two plots above, it is evident that the optimization favors larger fill spacing and smaller warp spacing, supporting the theoretical expectation that greater warp reinforcement is beneficial under bending loads. Additionally, the mass versus strain plot shows clustering around 100 grams and approximately 3000 $\mu\varepsilon$, reflecting the imposed strain constraint during optimization.

5.6 Summary of Optimization Results

The final lattice design emerged from a structured process combining DOE, surrogate modeling, and constrained optimization. Initial sampling via Latin Hypercube provided sufficient coverage of the design space. Using this dataset, a Sampling Fit surrogate model captured the influence of spacing, width, and thickness variables on strain and mass.

HyperStudy's Global Response Surface Method (GRSM) was employed for optimization.

GRSM balances global search and local refinement, avoiding premature convergence and identifying stable solutions well within constraint boundaries.

The algorithm successfully removed unnecessary fill reinforcement, confirming theoretical expectations that warp-direction tapes dominate in 3-point bending. The transition toward a sparse lattice structure reduced mass by approximately 21% compared to the baseline continuous panel, while remaining within the imposed strain constraint of 3430 $\mu\varepsilon$.

This configuration achieves a mass reduction of approximately 21% compared to the baseline panel while satisfying the strain constraint. For aerospace applications, such a weight saving at the panel level can scale to significant reductions in overall structural mass, improving fuel efficiency and payload capacity.

These results validate the use of classical optimization strategies even for architected composite systems when homogenized material models are used. The convergence to a lightweight, manufacturable design demonstrates that multiscale surrogate-based optimization can guide effective structural simplification.

Table 5.3: Optimal lattice configuration from refined optimization study

Parameter	**Optimal Value**
WARP_SPAC	0.08
FILL_SPAC	96.68
Mass (g)	109.56
Strain ($\mu\varepsilon$)	3311

5.6.1 What Makes HyperStudy Pick This Iteration as "Optimal"

The optimal configuration in Table 5.3 was selected by HyperStudy through a balance of surrogate model accuracy, objective minimization, and constraint satisfaction. The surrogate model achieved overall coefficients of determination of $R^2 = 0.95$ for the strain response and $R^2 = 0.97$ for the mass response, ensuring that the Global Response Surface Method (GRSM) could explore the design space with high confidence in predicted values.

While these R^2 values describe the global fit quality, each design point also has its own local surrogate accuracy. HyperStudy tracks these individual R^2 values to ensure the optimizer does not converge on regions where the surrogate fit is weak. This prevents the selection of points where predicted responses may be unreliable, even if they appear optimal in the surrogate surface.

During the optimization, several designs offered similar mass values, but many were rejected for exceeding the tensile strain limit of 3430 $\mu\epsilon$. The selected configuration minimized mass while keeping the strain at 3311 $\mu\epsilon$, comfortably within the limit and located in a region where small changes in warp or fill spacing would not push the design into violation. HyperStudy's approach inherently avoids extreme edge cases in the design space, favoring robust solutions that maintain performance under slight parameter variations.

Figure 5.12 shows the evaluated designs plotted in terms of mass and maximum tensile strain, with each point colored by its local surrogate R^2 accuracy for the strain prediction. Warmer colors indicate higher predictive accuracy. The dashed line marks the strain constraint, and the red marker highlights the chosen design — one of the lowest-mass feasible configurations with high surrogate accuracy and a safe margin below the strain limit.

5.7 Limitations

While the proposed multiscale optimization framework provides a practical and computationally efficient approach for composite lattice analysis, several limitations remain that should be acknowledged.

1. Linear Static Analysis

The current study utilizes linear static simulations only. This restricts its ability to capture large-deformation behavior, nonlinear stress–strain relationships, or post-yield phenomena. As such, results may not accurately reflect performance under crash, buckling, or impact loading.

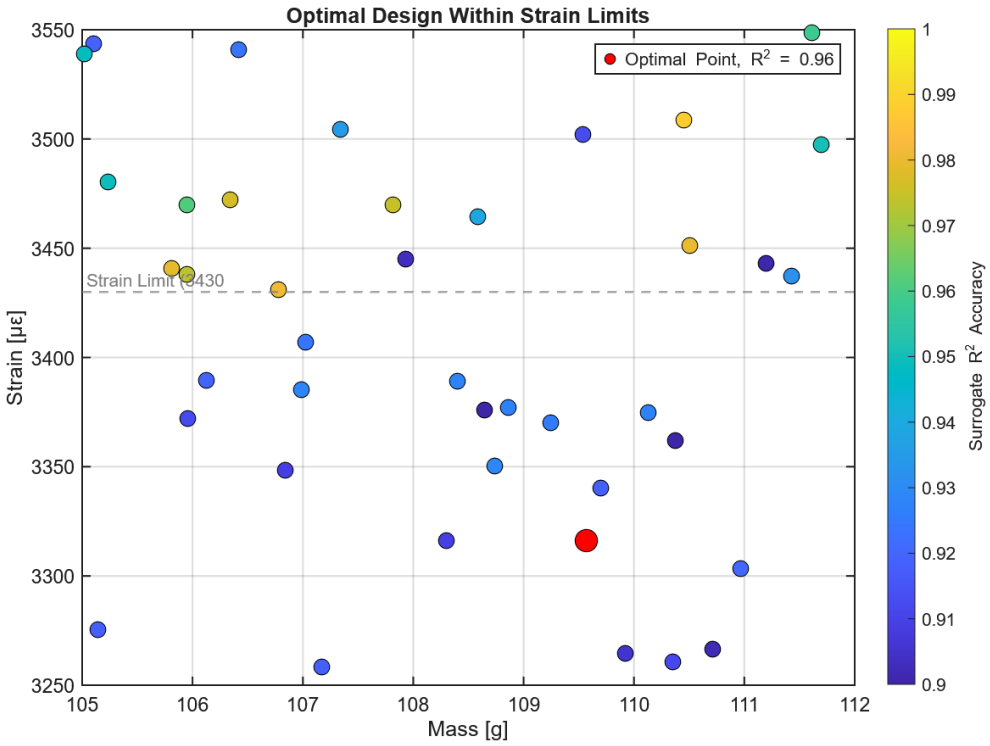

Figure 5.12: Distribution of evaluated design points in terms of mass and maximum tensile strain. Colors indicate local surrogate R^2 accuracy for strain prediction. The dashed line marks the strain constraint of 3430 $\mu\epsilon$. The red marker shows the selected optimal design, combining low mass, constraint satisfaction, and high surrogate accuracy.

2. No Progressive Damage or Failure Modeling

The homogenized material models used do not include damage progression or ultimate failure behavior. This limits the predictive capability for long-term durability, fatigue performance, or behavior near critical stress thresholds.

3. Surrogate Model Accuracy

The Sampling Fit surrogate model, although highly accurate in predictions, inherently introduces approximation errors that may slightly deviate from actual behavior.

4. Manufacturability Not Formally Enforced

Although input parameter bounds were selected based on realistic values for tape width, spacing, and fiber volume fractions, manufacturability constraints were not directly enforced within the optimization routine. Some resulting configurations may be difficult or costly to fabricate using current Weav3D systems.

5. Limited Experimental Validation

While the material properties were validated, the actual results were simulated. A full-scale experimental campaign on these lattice structures was not conducted. As a result, the predictive accuracy of the optimized configurations under real manufacturing imperfections, environmental effects, and variable load states remains to be demonstrated.

5.8 Future Work

While this study demonstrates a robust framework for composite lattice optimization, several avenues exist for extending its scope and improving its industrial applicability.

1. Nonlinear and Damage Modeling

Current simulations are based on linear static analysis. Future work should integrate nonlinear analysis capabilities, including geometric and material nonlinearity. Incorporating damage models such as cohesive zone models or continuum damage mechanics would allow accurate failure prediction under crash and impact loading [38].

2. Variable Lattice Architectures

The optimization assumes uniform lattice configurations across the structure. However, recent literature emphasizes the benefits of functionally graded lattice structures that vary tape density, orientation, or material based on load paths [58]. Implementing spatially varying designs could further improve stiffness-to-weight ratios in critical areas.

3. Machine Learning-Aided Optimization

Integrating artificial intelligence into the optimization process offers potential gains in efficiency. Physics-informed neural networks (PINNs) have shown promise in accelerating multiscale topology optimization problems by learning solution behavior from data [20]. Incorporating such techniques can reduce solver calls and increase the tractability of high-dimensional problems.

4. Manufacturability Constraints

While manufacturability was qualitatively considered, future studies should formally encode constraints like minimum spacing, toolpath curvature, and process-induced defects directly within the optimization problem. This will help bridge simulation and production more closely.

5. Experimental Validation

A natural extension of this work involves validating simulation outcomes through physical experiments. Fabricating optimized samples and testing their performance under standardized conditions would strengthen the modeling assumptions and support adoption in real applications.

6. Multi-Objective Optimization

This thesis used a single-objective framework. Future work should explore multi-objective formulations balancing stiffness, strength, cost, and manufacturability.

5.9 Final Conclusions

This thesis developed a computational framework for optimizing composite lattice structures and showed clear performance advantages over continuous composite designs. Using Latin Hypercube Sampling, the design space was explored broadly, and a surrogate model was built to capture the key relationships between design parameters and structural responses. This model greatly reduced computational cost while still providing accurate predictions.

Optimization with Altair HyperStudy's Global Response Surface Method (GRSM) demonstrated that widening warp and fill spacings shifts the structure toward an efficient lattice configuration. The best design reduced the panel weight from about 138 grams to 109 grams (a 21% improvement) while keeping strain within the target limit of about 3000 $\mu\varepsilon$. The algorithm consistently removed non-critical fill reinforcement while retaining closely spaced warp tows, reflecting the dominant load path in bending. Similar weight savings have been reported by Wollschlager and Oberste, supporting the validity of these results, with this work adding the contribution of a fully automated, surrogate-based workflow.

These findings support the central idea of lattice composites: placing reinforcement only where it is structurally needed can deliver lightweight and efficient designs. The work also confirms Weav3D's core principle that lattice geometry can be tuned to cut mass without sacrificing performance.

While the study relied on simplifying assumptions such as homogenization, linear elasticity, and no manufacturing constraints, the results remained robust and practically meaningful.

Future efforts should focus on physical validation of the optimized lattices, extending the models to capture nonlinear and dynamic loading, and integrating realistic manufacturing limits. With these steps, the approach can become a practical tool for designing advanced lightweight structures in aerospace, automotive, and other demanding fields.

BIBLIOGRAPHY

[1] *Weav3D, Inc. "Materials"* https://weav3d.com/materials *(Accessed April 9, 2025).* Accessed April 9, 2025.

[2] Astm d3039/d3039m-17: Standard test method for tensile properties of polymer matrix composite materials. ASTM International, 2017. Accessed: December 2024.

[3] Astm d3518/d3518m-18: Standard test method for in-plane shear response of polymer matrix composite materials by tensile test of a ±45° laminate. ASTM International, 2018. Accessed: December 2024.

[4] *WEAV3D, Inc. "Technology Overview."* https://www.weav3d.com/technology *(Accessed April 9, 2025).*

[5] FS Almeida and AM Awruch. Design optimization of composite laminated structures using genetic algorithms and finite element analysis. *Composite structures*, 88(3):443–454, 2009.

[6] Altair Engineering Inc. *HyperStudy Help: Global Response Surface Method (GRSM)*, 2021. Accessed: December 2024.

[7] Altair Engineering Inc. *HyperStudy Help: Latin Hypercube Sampling (DOE Method)*, 2021. Accessed: December 2024.

[8] Altair Engineering Inc. *OptiStruct Bulk Data: MAT2*, 2021. Accessed: December 2024.

[9] Altair Engineering Inc. *OptiStruct Bulk Data: PSHELL*, 2021. Accessed: December 2024.

[10] M.J. Anderson. *DOE Simplified: Practical Tools for Effective Experimentation, Third Edition.* Taylor & Francis, 2017.

[11] Ziad K Awad, Thiru Aravinthan, Yan Zhuge, and Felipe Gonzalez. A review of optimization techniques used in the design of fibre composite structures for civil engineering applications. *Materials & Design*, 33:534–544, 2012.

[12] Christopher Cameron, Dženan Hozić, Fredrik Stig, and Sjoerd van der Veen. A method for optimization against cure-induced distortion in composite parts. *Structural and Multidisciplinary Optimization*, 66(51), 2023.

[13] Adrian Chapple, Zidane Tahir, and Fraser Jardine. Weld distortion optimisation using hyperstudy. In *The 8th UK Altair technology conference*, pages 1–13, 2013.

[14] Nicholas P. Cheremisinoff and Paul N. Cheremisinoff. *Fiberglass Reinforced Plastics*. William Andrew Publishing, 1995.

[15] Norman R. Draper and Harry Smith. *Applied Regression Analysis*. Wiley, New York, 3 edition, 1998. Standard reference for regression and derivation of the coefficient of determination (R^2).

[16] Advanced Engineering. Introduction into design of experiments (doe) with hyperstudy. https://advanced-eng.cz/wp-content/uploads/2021/06/2021_ebook-HyperStudy.pdf, 2021.

[17] Advanced Engineering. Practical aspects of structural optimization with altair optistruct. https://www.advanced-eng.cz/wp-content/uploads/2021/06/ebook_Practical_Aspects_of_Optimization_with_Altair_OptiStruct_2021.pdf, 2021.

[18] Altair Engineering. Composite optimization in hyperstudy. https://community.altair.com/discussion/11152/composite-optimization-in-hyperstudy, 2018.

[19] Altair Engineering. Design, analyze, and simulate advanced composite structures. https://altair.com/composites/, 2020.

[20] Yiming Feng, Thien Nguyen, and Yu Wang. Pinn-accelerated multiscale topology optimization using physics-informed neural networks. *arXiv preprint arXiv:2408.00510*, 2024.

[21] A. Ghazlan et al. Multi-level optimisation of composite structures through a global–local approach. *Computers Structures*, 260:106–117, 2022.

[22] L.J. Gibson and M.F. Ashby. Design and optimization of lattice structures: A review. *Applied Sciences*, 10(18):6374, 2020.

[23] Zafer Gürdal, Raphael T Haftka, and Prabhat Hajela. *Design and optimization of laminated composite materials*. John Wiley & Sons, 1999.

[24] F. J. Hickernell and H. Niederreiter. Monte carlo and quasi-monte carlo methods. In *Monte Carlo and Quasi-Monte Carlo Methods*, pages 1–10. Springer, 2003. Describes lattice sequences and extensible lattice rules, foundational for Modified Extensible Lattice Sequences (MELS).

[25] Fred J. Hickernell, Hee Sun Hong, Pierre L'Écuyer, and Christiane Lemieux. Extensible lattice sequences for quasi-monte carlo quadrature. *SIAM Journal on Scientific Computing*, 22(3):1117–1138, 2000.

[26] D.E. Huntington and C.S. Lyrintzis. Improvements to and limitations of latin hypercube sampling. *Probabilistic Engineering Mechanics*, 13(4):245–253, 1998.

[27] Altair Engineering Inc. Bulk data section — optistruct. `https://help.altair.com/2021/hwsolvers/os/topics/solvers/os/bulk_data_section.htm`, 2021. Accessed: January 2025.

[28] Robert M. Jones. *Mechanics of Composite Materials (2nd ed.)*. CRC Press, 1999.

[29] Alexander L Kalamkarov and Alexander G Kolpakov. *Analysis, design and optimization of composite structures*, volume 1. Wiley New York, 1997.

[30] Meghana Kamble, Robert Jopson, Jeffrey Wollschlager, and Christopher Oberste. Composite lattice reinforced part optimization with fea: An automotive door component case study. 2024.

[31] P. Kanouté, D.P. Boso, J.L. Chaboche, and B.A. Schrefler. Multiscale methods for composites: A review. *Archives of Computational Methods in Engineering*, 16(1):31–75, 2009.

[32] Jack P. C. Kleijnen. *Response Surface Methodology*. Springer New York, New York, NY, 2015.

[33] Guanghui Lan. An optimal method for stochastic composite optimization. *Mathematical Programming*, 133(1):365–397, 2012.

[34] Jean Laurenceau and Thomas Allen. Comparison of gradient and response-surface based optimization frameworks using adjoint method. *AIAA Journal*, 48(5):981–994, 2010.

[35] J. Lemaitre and R. Desmorat. Progressive damage modeling in fiber-reinforced materials. *Composites Part B: Engineering*, 38(2):221–233, 2007.

[36] Z. Liu, H. Wei, and C.T. Wu. Multiscale modeling of composite materials under volumetric and shear loading. In *AIAA Scitech 2023 Forum*, pages 1–12. American Institute of Aeronautics and Astronautics, 2023.

[37] Wei-Liem Loh. On latin hypercube sampling. *The annals of statistics*, 24(5):2058–2080, 1996.

[38] Xin Lu, Ryo Higuchi, and Tomohiro Yokozeki. Adaptive implicit–explicit method for robust and efficient failure analysis of composite materials. *Composites Part A: Applied Science and Manufacturing*, 180:108093, 2024.

[39] Zhifan Luo. Benchmark of hyperstudy optimization algorithms. Technical report, Altair Engineering, 2015.

[40] Nick McCormick and Jerry Lord. Digital image correlation. *Materials Today*, 13(12):52–54, 2010.

[41] M. D. McKay, R. J. Beckman, and W. J. Conover. A comparison of three methods for selecting values of input variables in the analysis of output from a computer code. *Technometrics*, 21(2):239–245, 1979.

[42] Christopher Oberste Meghana Kamble. A novel fea approach to design and optimize composite latticereinforcements and simulate the mechnical properties of composite lattice reinforced plastics. *CAMX-The Composites and Advanced Materials Expo*, 2024.

[43] A Muc and W Gurba. Genetic algorithms and finite element analysis in optimization of composite structures. *Composite Structures*, 54(2-3):275–281, 2001.

[44] André Mönicke, Harri Katajisto, and Robert Yancey. Design optimization of a curved layered composite panel using efficient laminate parameterization. In *SAMPE Long Beach 2016 Conference Proceedings*. Society for the Advancement of Material and Process Engineering, 2016.

[45] Nico JD Nagelkerke et al. A note on a general definition of the coefficient of determination. *biometrika*, 78(3):691–692, 1991.

[46] Christopher Oberste. Investigating the relationship between fiber length, volume fraction, and mechanical properties of fiber-reinforced plastics, 2019.

[47] Christopher M. Oberste. *Design, modelling, and fabrication of interlaced thermoplastic composites by additive manufacturing*. Ph.d. dissertation, Georgia Institute of Technology, Atlanta, GA, 2017.

[48] Christopher M Oberste and Meghana Kamble. Rebar for plastics–a novel approach to part optimization with composite lattices. 2023.

[49] Anders M. J. Olsson and Göran E. Sandberg. Latin hypercube sampling for stochastic finite element analysis. *Journal of Engineering Mechanics*, 128(1):121–125, 2002.

[50] Robin Preece and Jovica Milanović. Efficient estimation of the probability of small-disturbance instability of large uncertain power systems. *IEEE Transactions on Power Systems*, 30(6):2971–2979, 2015.

[51] Y. Qiao and Marco Salviato. Strength and cohesive behavior of thermoset polymers at the microscale: A size-effect study. *arXiv preprint*, arXiv:1812.05732, 2018.

[52] Y. Qiao and Marco Salviato. Study of the fracturing behavior of thermoset polymer nanocomposites via cohesive zone modeling. *arXiv preprint*, arXiv:1808.09787, 2018.

[53] Nestor V. Queipo, Raphael T. Haftka, Wei Shyy, Tushar Goel, Rajkumar Vaidyanathan, and Piyush Kevin Tucker. Surrogate-based analysis and optimization. *Progress in Aerospace Sciences*, 41(1):1–28, 2005.

[54] A. Sabsabi, M. A. Youssef, O. El-Azizy, and M. Kamble. Numerical modeling of the bond behavior between thermoplastic frp lattice and concrete. In Rishi Gupta, Min Sun, Svetlana Brzev, M. Shahria Alam, Kelvin Tsun Wai Ng, Jianbing Li, Ashraf El Damatty, and Clark Lim, editors, *Proceedings of the Canadian Society of Civil Engineering Annual Conference 2022*. Springer Nature Switzerland, 2023.

[55] Timothy W. Simpson, Jaroslaw D. Poplinski, Paul N. Koch, and Janet K. Allen. Metamodels for computer-based engineering design: survey and recommendations. *Engineering with Computers*, 17(2):129–150, 2001. Foundational survey on surrogate modeling and the Global Response Surface Method (GRSM).

[56] Six Sigma US. Response surface methodology (rsm), 2022. Accessed: 2025-07-28.

[57] András Sóbester, Stephen J. Leary, and Andy J. Keane. On the design of optimization strategies based on global response surface approximation models. *Journal of Global Optimization*, 33(1):31–59, 2005.

[58] Mohammad Torabi, Lei Zhang, and Xi Chen. Multi-scale modeling of graded composite lattices for structural applications. *Computer Methods in Applied Mechanics and Engineering*, 419:116034, 2024.

[59] G. Totaro and Z. Gürdal. Optimal design of composite lattice shell structures for aerospace applications. *Aerospace Science and Technology*, 13(4):157–164, 2009.

[60] Y. Wang, X. Sun, and Y. Li. Progressive damage analysis of composite structures using higher order shear deformation theory. *Composites Part B: Engineering*, 173:106–115, 2019.

[61] Jeffrey A Wollschlager, Chris Oberste, Meghana Kambel, and Marco Salviato. A multiscale approach to the design and analysis of WEAV3D lattice structures. *CAMX-The Composites and Advanced Materials Expo*, 2024.

[62] Y. Zhang, X. Wang, and J. Li. Multiscale modelling of composite laminates with voids through the representative volume element approach. *Composite Structures*, 300:116–125, 2024.

[63] Ming Zhou, Raphael Fleury, and Martin Kemp. Optimization of composite-recent advances and application. In *13th AIAA/ISSMO multidisciplinary analysis optimization conference*, page 9272, 2010.